Arabidopsis PHOSPHOTYROSYL PHOSPHATASE ACTIVATOR Is Essential for PROTEIN PHOSPHATASE 2A Holoenzyme Assembly and Plays Important Roles in Hormone Signaling, Salt Stress Response, and Plant Development[1][W][OPEN]

Jian Chen, Rongbin Hu, Yinfeng Zhu, Guoxin Shen*, and Hong Zhang*

Department of Biological Sciences, Texas Tech University, Lubbock, Texas 79409 (J.C., R.H., Y.Z., G.S., H.Z.); and Zhejiang Academy of Agricultural Sciences, Hangzhou, Zhejiang Province 310021, China (G.S.)

PROTEIN PHOSPHATASE 2A (PP2A) is a major group of serine/threonine protein phosphatases in eukaryotes. It is composed of three subunits: scaffolding subunit A, regulatory subunit B, and catalytic subunit C. Assembly of the PP2A holoenzyme in Arabidopsis (*Arabidopsis thaliana*) depends on Arabidopsis PHOSPHOTYROSYL PHOSPHATASE ACTIVATOR (AtPTPA). Reduced expression of *AtPTPA* leads to severe defects in plant development, altered responses to abscisic acid, ethylene, and sodium chloride, and decreased PP2A activity. In particular, *AtPTPA* deficiency leads to decreased methylation in PP2A-C subunits (PP2Ac). Complete loss of PP2Ac methylation in the *suppressor of brassinosteroid insensitive1* mutant leads to 30% reduction of PP2A activity, suggesting that PP2A with a methylated C subunit is more active than PP2A with an unmethylated C subunit. Like AtPTPA, PP2A-A subunits are also required for PP2Ac methylation. The interaction between AtPTPA and PP2Ac is A subunit dependent. In addition, *AtPTPA* deficiency leads to reduced interactions of B subunits with C subunits, resulting in reduced functional PP2A holoenzyme formation. Thus, AtPTPA is a critical factor for committing the subunit A/subunit C dimer toward PP2A heterotrimer formation.

Phosphorylation and dephosphorylation of proteins is a universal mechanism for the regulation of diverse biological functions (Hunter, 1995). PROTEIN PHOSPHATASE 2A (PP2A) enzymes account for the majority of Ser/Thr phosphatase activity in eukaryotic cells. These enzymes exist as heterotrimer holoenzymes that include a scaffolding A subunit, a regulatory B subunit, and a catalytic C subunit (Janssens and Goris, 2001; DeLong, 2006). The existing model for PP2A holoenzyme formation suggests that the structurally conserved catalytic subunit C associates with the highly conserved subunit A to form an AC dimer, and the AC dimer then interacts with a B subunit to form the ABC heterotrimer (Janssens and Goris, 2001). In plants, PP2A was found to be involved in the signal transduction pathways of several hormones, including abscisic acid (ABA; Kwak et al., 2002; Pernas et al., 2007), auxin (Garbers et al., 1996; Michniewicz et al., 2007), and ethylene (Larsen and Chang, 2001; Muday et al., 2006; Skottke et al., 2011).

Two A subunits of PP2A exist in mammals, and they are named PUTATIVE REGULATORY 65A (PR65A) and PR65B. These two A subunits consist of 15 HEAT (for Huntingtin, elongation factor3, a subunit of PP2A, phosphatidylinositol3 kinase target of rapamycin1) repeats (Hemmings et al., 1990). The first PR65 ortholog identified in Arabidopsis (*Arabidopsis thaliana*) represents one of the three A subunits (i.e. A1) and is encoded by the gene *ROOT CURLS IN NAPHTHYLPHTHALAMIC ACID1* (*RCN1*; Garbers et al., 1996) or *ENHANCED ETHYLENE RESPONSE1* (*EER1*; Larsen and Chang, 2001). The mutant *rcn1-1* was shown to have an enhanced response to the auxin transport inhibitor naphthylphthalamic acid, which led to increased accumulation of free indole-3-acetic acid in the apical meristem (Garbers et al., 1996). This result suggested that RCN1 plays an essential role in auxin transport, which was later confirmed by Michniewicz et al. (2007). The *rcn1-1* mutant was also found to be salt sensitive

(Blakeslee et al., 2008), indicating that RCN1 is also involved in salt signaling in plants. In addition, *rcn1* mutants were found to confer ABA insensitivity during seed germination (Kwak et al., 2002) and enhanced responsiveness to ethylene (Larsen and Chang, 2001). While evidence from the study of *rcn1* mutants shows that PP2A plays important roles in plant growth and development, hormone signaling, and stress response pathways, the specific role of this A1 subunit in PP2A holoenzyme assembly in plants is less well understood.

Five genes that encode PP2A catalytic subunits (PP2Ac) are found in Arabidopsis, and these five C subunits are grouped into two subfamilies: subfamily I (PP2A-C1, PP2A-C2, and PP2A-C5) and subfamily II (PP2A-C3 and PP2A-C4; Pérez-Callejón et al., 1998). Members of subfamily I are believed to be involved in plant stress and defense responses (He et al., 2004). Virus-induced gene silencing of the PP2Ac subfamily I in *Nicotiana benthamiana* led to increased plant defense responses and localized cell death (He et al., 2004). A null mutant of the *PP2A-C2* gene in Arabidopsis is hypersensitive to both ABA and NaCl (Pernas et al., 2007). País et al. (2009) demonstrated that transcripts of the subfamily I genes are down-regulated by cold in tomato (*Solanum lycopersicum*). Members of PP2Ac subfamily II are likely to be involved in auxin transport, as *pp2a-c3c4* double mutants are not viable and have altered auxin distribution patterns (Ballesteros et al., 2013). Consistent with studies on *rcn1* mutants, work with PP2Ac also suggests the involvement of PP2A in crucial developmental processes and stress responses in plants.

The final six amino acid residues at the C terminus of eukaryotic PP2Ac are highly conserved. Leu-309 at the carboxyl end can be extensively methylated, and this methylation plays an important role in controlling PP2A activity (Wu et al., 2000; Stanevich et al., 2011). The methylation reaction at this site is catalyzed by LEUCINE CARBOXYLMETHYL TRANSFERASE1 (LCMT1). It was estimated that 50% to 90% of Leu-309 in PP2Ac is methylated in eukaryotic cells (Kalhor et al., 2001; Wu et al., 2011). Methylation of PP2Ac is not detectable in the Arabidopsis *LCMT1*-null mutant known as *suppressor of brassinosteroid insensitive1* (*sbi1-1*), indicating that SBI1 is likely to be the primary PP2Ac methylating enzyme in Arabidopsis (Wu et al., 2011). The unmethylated PP2Ac form was 5- to 10-fold more abundant in the *sbi1-1* mutant than in wild-type plants, suggesting that 80% to 90% of PP2Ac are methylated in Arabidopsis (Wu et al., 2011). While loss of methylation in PP2Ac in yeast (*Saccharomyces cerevisiae*) led to developmental defects (Wu et al., 2000; Wei et al., 2001), the Arabidopsis *sbi1-1* mutant was viable and showed minimal morphological defects (Wu et al., 2011), suggesting that loss of PP2Ac methylation is not detrimental to plant development.

There are at least 17 regulatory B subunits in Arabidopsis, and these subunits are subcategorized into three different groups: B, B′, and B′′ (Farkas et al., 2007). It is well understood that B subunits are responsible for selecting various PP2A substrates. Recent work with B subunits revealed diverse PP2A substrates, which begins to show how PP2A may be involved in several developmental and hormonal processes (Heidari et al., 2011; Leivar et al., 2011; Tang et al., 2011). In addition to the association with the regulatory B subunits, PP2Ac subunits were also found to interact with a noncanonical regulatory subunit known as PHOSPHOTYROSYL PHOSPHATASE ACTIVATOR (PTPA; Ogris et al., 1999). PTPA was first isolated from rabbit skeletal muscle (Cayla et al., 1990), and it was able to reactivate an inactive form of PP2A via an ATP/Mg^{2+}-dependent mechanism (Ogris et al., 1999; Longin et al., 2004). While PTPA was originally thought to be a putative regulatory B subunit due to its ability to associate with the AC dimer (Fellner et al., 2003), studies showed that PTPA could activate PP2A Tyr phosphatase activity with the Tyr substrate mimic *p*-nitrophenylphosphate in vitro (Cayla et al., 1990). Although PP2A is generally considered to be a Ser/Thr phosphatase, in vitro Tyr phosphatase activity was reported for PP2As derived from animal cells (Chen et al., 1992). However, Tyr phosphatase activity has yet to be shown with plant PP2As. Hombauer et al. (2007) showed that PTPA orthologs in yeast known as RESISTANCE TO RAPAMYCIN DELETION1 (RRD1) and RRD2 play a critical role in the PP2A holoenzyme assembly. This work corroborated earlier evidence that PTPA from animal cells facilitates PP2A holoenzyme formation (Fellner et al., 2003). In particular, their work demonstrated the interaction between PTPA and PP2Ac and showed that PTPA prefers to bind to an active-site mutant over wild-type PP2Ac. Jordens et al. (2006) proposed that PTPA functions as a novel peptidyl-prolyl cis/trans-isomerase. Analysis of the crystal structures of native and mutant PTPAs also supports the idea that PTPA causes specific conformation changes in PP2Ac (Leulliot et al., 2006). Another structural study from Chao et al. (2006) revealed that PTPA could interact with AC dimers and form a composite ATPase that is likely to be required for the PTPA-dependent change in PP2A substrate specificity in vitro. Another recent study suggests that PTPA acts as a molecular chaperone and that ATP hydrolysis by the composite ATPase is crucial for specific Ser/Thr substrate selection by PP2A (Guo et al., 2014). Although the role of PTPA in yeast and animal cells is being uncovered, nothing is known about the functions of PTPA in plants.

In this study, we used the artificial microRNA (amiRNA) technique to down-regulate the expression of *AtPTPA*, a PTPA ortholog in Arabidopsis, and studied the biological consequences of *AtPTPA* deficiency in plants. AtPTPA deficiency led to nearly complete loss of Leu-309 methylation in PP2Ac, with more loss of PP2A activity than in *sbi1* mutant plants. This finding indicates that the action of AtPTPA on PP2Ac may be required before PP2Ac is methylated by SBI1 in plants. Protein-protein interaction analysis revealed that the action of AtPTPA on PP2Ac is A subunit dependent, indicating the existence of a PP2A-A/AtPTPA/PP2A-C trimer. In addition, pull-down experiments showed that

the interactions between B subunits (i.e. ATB′ η and ATB′ γ) and PP2Ac were both decreased in *AtPTPA* knockdown plants. Overall, our work indicates that AtPTPA is a critical regulator for PP2A holoenzyme assembly in plants.

RESULTS

Expression Pattern of *AtPTPA* in Arabidopsis

The Arabidopsis PTPA ortholog is encoded by a single gene (At4g08960), and database searches revealed no genes that share significant sequence similarities in the Arabidopsis genome. This Arabidopsis PTPA gene *AtPTPA* encodes a putative protein that displays 40% identity to human PTPA, about 40% identity to the yeast PTPA orthologs RRD1 and RRD2, and 60% identity to a putative PTPA ortholog from rice (*Oryza sativa*; Supplemental Fig. S1). To investigate the function of *AtPTPA* in Arabidopsis, the expression pattern of *AtPTPA* was studied using a reporter gene in transgenic plants. The 5′ flanking sequences of *AtPTPA*, along with 21 nucleotides of the *AtPTPA* coding sequence (−1,721 to +21), were fused, in frame, to the *GUS* gene (Fig. 1A). The resulting P_{AtPTPA}::*GUS* construct was introduced into Arabidopsis using the floral dip transformation method (Clough and Bent, 1998), and 30 independent transgenic lines were generated. All primary transgenic plants were allowed to self-pollinate to reach the T3 generation. Based on segregation analysis of the kanamycin resistance phenotype, eight single transfer DNA (T-DNA) insertion homozygous lines were chosen for histochemical staining analysis. One representative example from the GUS staining data is shown in Figure 1B.

Three-day-old seedlings grown on Murashige and Skoog (MS) medium did not show any GUS staining. However, 6-d-old seedlings displayed strong GUS staining in the emerging lateral roots but not in the main root (Fig. 1Bc). Weak signal was also detected in hypocotyls. In 5-week-old plants, GUS staining was found mainly in the vascular tissues of leaf, root, and stem (Fig. 1, Ba, Bf, and Bg). Strong GUS staining was found in leaf veins but not in mesophyll cells (Fig. 1Ba). Moreover, unlike in young seedlings, strong GUS staining was found in the entire root systems (Fig. 1Bf). In the reproductive tissues, extensive GUS staining was found in inflorescence and developing siliques (Fig. 1Bb). Similar results were observed when a stained flower was examined with the microscope (Fig. 1, Bd and Be). Overall, the histochemical staining results showed that *AtPTPA* was expressed in most tissues throughout plant growth and development.

To corroborate the GUS staining pattern, RNA-blot analysis was performed by using a ^{32}P-labeled *AtPTPA* complementary DNA (cDNA) as the probe. A single hybridizing band of about 1.5 kb was detected in RNA samples isolated from most organs (Fig. 1C). Consistent with the GUS staining data, the *AtPTPA* transcript
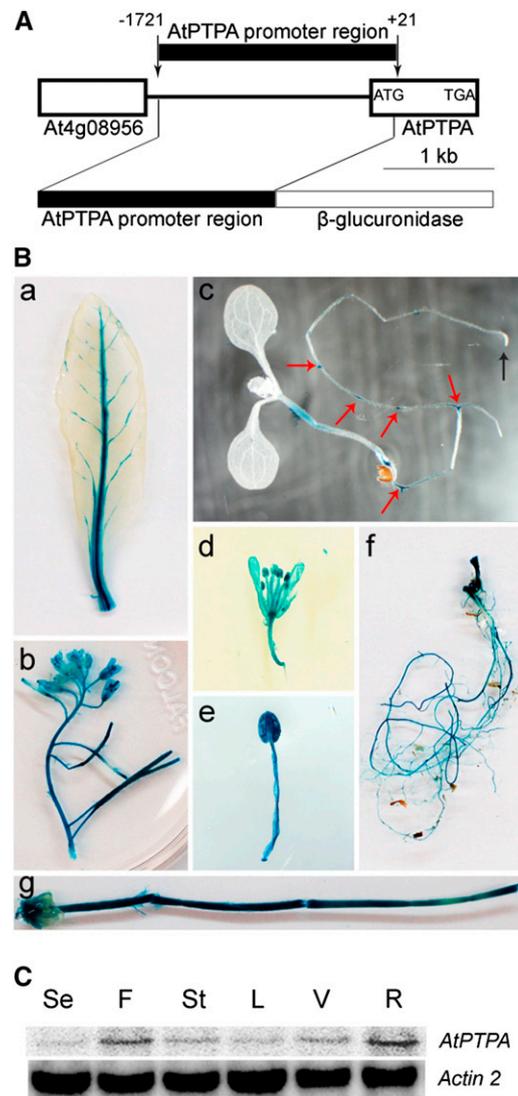

Figure 1. Creation of the P_{AtPTPA}::*GUS* fusion construct and the expression pattern of *AtPTPA* in Arabidopsis. A, *AtPTPA* promoter information. The 5′ sequence of *AtPTPA* from −1,721 to +21 bp was translationally fused to the *GUS* gene. B, Histochemical staining pattern of P_{AtPTPA}::*GUS* transgenic plants: a, rosette leaf; b, flowers and siliques; c, 6-d-old seedling; d, flower; e, stamen; f, root system; and g, stem. Red arrows indicate the newly emerged lateral roots, while the black arrow indicates the main root tip. C, RNA-blot analysis of *AtPTPA* in Arabidopsis tissues. Se, Seedlings; F, flowers; St, stem; L, rosette leaves; V, veins from leaves; R, roots. *ACTIN2* was used as the loading control.

was found at relatively high levels in flowers and roots (Fig. 1C). Weak signals were detected in 6-d-old seedlings and 4-week-old leaves. Moreover, the RNAs from the leaf veins showed enriched *AtPTPA* transcript compared with those from total leaves. Taken together, our results provide evidence that *AtPTPA* is expressed in most tissues and, in particular, that high expression of *AtPTPA* occurs in developing lateral root and in reproductive tissues.

AtPTPA Is Essential for Plant Growth and Development

Because there were no T-DNA-tagged *AtPTPA* mutants available, we created transgenic plants with the amiRNA technique to down-regulate *AtPTPA* expression. The amiRNA against *AtPTPA* was created by using software from the small RNA designer WMD3 (Schwab et al., 2006). The amiRNA sequence (Fig. 2A) was first inserted into the binary vector and then introduced into wild-type Arabidopsis. The majority of the independent transgenic amiR-expressing plants, 38 out of 46, were substantially smaller than wild-type plants at week 4 and had relatively dark green rosette leaves (Fig. 2B). The amiR plants also showed early senescence of cotyledons and the first pair of true leaves (Fig. 2B). Three amiR transgenic lines in the wild-type background, amiR-10 (WT), amiR-6 (WT), and amiR-4 (WT), were chosen for further molecular analysis after homozygous lines were obtained at the T3 generation. Two lines, amiR-6 (WT) and amiR-4 (WT), were chosen for further physiological analysis. As shown in Figure 2C, all three transgenic lines showed nearly total loss of *AtPTPA* transcript, indicating the high efficiency of the amiRNA technique. However, the quantitative real-time (qRT)-PCR analysis showed that about 10% of *AtPTPA* transcripts were still found in these amiR plants (Supplemental Fig. S2). Immunoblot analysis with AtPTPA antibodies
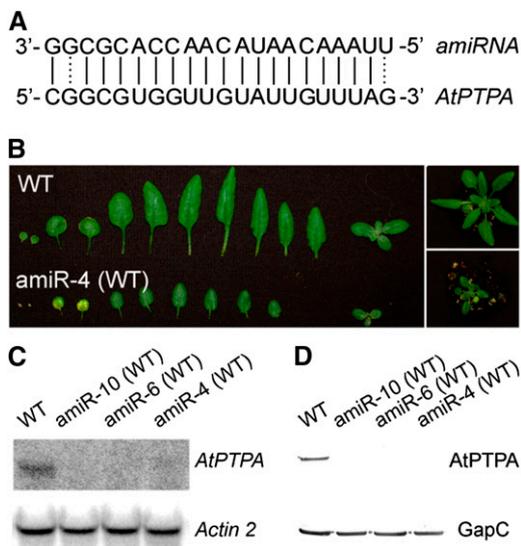
Figure 2. Creation and analysis of amiR plants. A, The amiRNA sequence (top strand) was used to regulate the target sequence of *AtPTPA* (bottom strand). Solid lines indicate perfect matches, and dashed lines indicate mismatches. B, Leaf comparison between a wild-type plant (WT) and an amiR plant. Both plants were 4 weeks old. C, RNA-blot analysis of wild-type and amiR plants. A cDNA fragment of *AtPTPA* was used as the probe, and *ACTIN2* was used as the RNA loading control. D, Western-blot analysis of wild-type and amiR plants. AtPTPA antibody was used to detect the AtPTPA protein, and cytosolic glyceraldehyde-3-phosphate dehydrogenase (GapC) was used as the protein loading control.

indicated that the steady-state level of AtPTPA was reduced by more than 90% (Fig. 2D). These data indicated that *AtPTPA* expression was reduced to below detectable levels in all three amiR plants. These data also showed that amiR plants with only 10% of the level of *AtPTPA* transcripts as wild-type plants were viable.

AtPTPA Deficiency Leads to Increased Sensitivity to ABA in Germination and Postgermination Growth

To test if *AtPTPA* is involved in ABA signaling pathways, the germination rates of two amiR plants, amiR-4 (WT) and amiR-6 (WT), were measured in the presence of ABA. Despite visible developmental defects (Fig. 2B), these plants germinated normally on MS medium. However, in the presence of 1 μM ABA, the germination rates of amiR plants were dramatically reduced (Fig. 3, A and B). Under these conditions, more than 50% of wild-type seeds germinated on day 3 and all germinated by day 4, yet only 55% to 80% of amiR plants germinated by day 7 (Fig. 3, A and B). At a higher concentration of ABA (2 μM), germination of amiR plants was even lower on day 7 (less than 40%), while all wild-type and *rcn1-6* seeds were germinated at this time (Fig. 3B). ABA is known to inhibit root development (Pilet and Saugy, 1987; Finkelstein et al., 2002); therefore, the main root growth of amiR plants in the absence or presence of ABA was analyzed. In the absence of ABA, the average root length of amiR plants (16 mm) was shorter than that of wild-type plants (22 mm). In the presence of ABA, the main root development of amiR plants was more severely inhibited than in wild-type plants. ABA inhibited main root growth in wild-type plants by 50% compared with growth on ABA-free MS medium (Fig. 3C), but it inhibited main root growth in amiR plants by 80% compared with growth on MS medium (Fig. 3C). These data indicate that *AtPTPA* is required for root development.

AtPTPA-Deficient Plants Are Also More Sensitive to Ethylene, Salt, and Cantharidin Treatments

Previous studies showed that *pp2a-a1* mutants such as *rcn1-6* and *eer1* display an enhanced response to ethylene and increased sensitivity to salt stress (Larsen and Chang, 2001; Muday et al., 2006; Blakeslee et al., 2008). Therefore, experiments were conducted to test how amiR plants would respond to salt and ethylene treatments. For the salt sensitivity test, 4-d-old seedlings were transferred to MS plates that contained either none or 100 mM NaCl. The plates were positioned vertically, and the plants were allowed to grow upside down for 3 d before root growth in the downward direction was measured. The root length was reduced by 50% in wild-type plants when compared with their growth on MS medium, while reductions of 60% to 70% were found in amiR plants (Fig. 4A). The salt overly
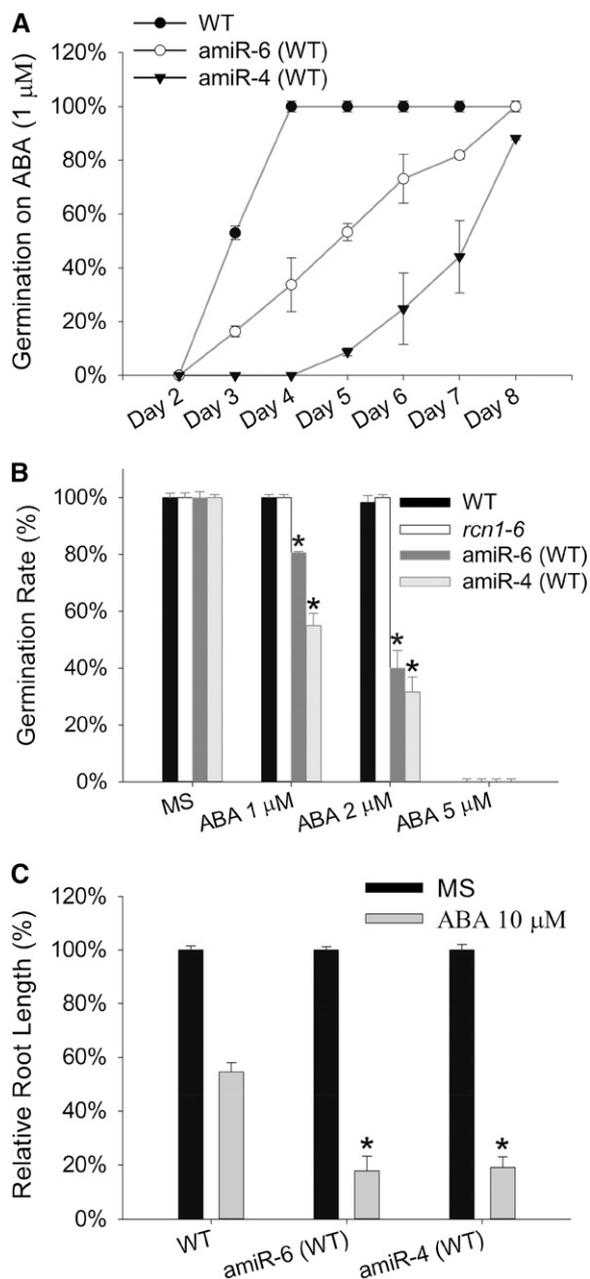
Figure 3. The amiR plants are more sensitive to ABA than wild-type plants at germination and postgermination stages. A, Germination rates of wild-type (WT) and two independent amiR plants on MS plates supplemented with 1 μM ABA. B, Germination rates of wild-type, *rcn1-6* mutant, and two independent amiR plants in the wild-type background on MS plates supplemented with different concentrations of ABA (1, 2, and 5 μM) on day 7. C, Relative main root length comparison (%) between ABA-treated and nontreated plants in wild-type and two independent amiR plants. Main root lengths were measured after 4-d-old seedlings were transferred onto MS plates supplemented with ABA (10 μM) or without ABA for 4 d. Error bars represent SD (*n* = 3). Asterisks indicate *P* < 0.01, as determined by Student's *t* test.

sensitive mutant *sos1-1* (Shi et al., 2000), a negative control in this assay, was more severely inhibited by 100 mM NaCl than plants of either amiR line.

For the ethylene response test, wild-type and amiR seeds were planted on MS plates that contained the ethylene precursor 1-aminocyclopropane-1-carboxylic acid (ACC) and allowed to germinate and grow vertically in darkness for 6 d before the hypocotyl length of wild-type and amiR plants was measured. Without ACC, similar to *rcn1-6* (19 mm), the hypocotyls of amiR plants (16 mm) were shorter than those of wild-type plants (24 mm). With ACC in the medium, the hypocotyls were reduced by 50% in wild-type plants, while the hypocotyls of amiR plants were reduced by 70% or more in comparison with their growth under ACC-free conditions (Fig. 4B). The ethylene-insensitive mutant *ein2-1* (Alonso et al., 1999), used as a control in this assay, was completely insensitive to ACC treatment.

The response of amiR plants to cantharidin, an inhibitor of PP2A and PP2A-related phosphatases such as PP6 (Li and Casida, 1992; Hu et al., 2014), was also analyzed. Four-day-old seedlings were transferred to MS plates that were not supplemented or were supplemented with 10 μM cantharidin, and plants were allowed to grow for an additional 4 d before the main root length was measured. As expected, root development in the PP2A mutant *rcn1-6* was more severely inhibited by cantharidin than that of wild-type plants (Fig. 4C). Similar to *rcn1-6* plants, root development of amiR plants was more severely inhibited by cantharidin than in wild-type plants. Taken together, these results indicate that reduced expression of *AtPTPA* in Arabidopsis leads to an enhanced response to ethylene and increased sensitivity to salt and cantharidin, which resembles the PP2A-A1 mutant *rcn1-6*. These results also suggest that *AtPTPA* deficiency could lead to impaired PP2A activity in plants.

Reduced Expression of *AtPTPA* in the *rcn1-6* Mutant Background Leads to More Severe Defects in Response to ABA, NaCl, Cantharidin, and ACC Treatments

To gain more insights into the role of *AtPTPA* in ABA, ethylene, and salt responses, *AtPTPA* expression was reduced in the *rcn1-6* background by introducing the same amiRNA construct into *rcn1-6* mutant plants. Three of the 30 independent lines generated, amiR-1 (*rcn1-6*), amiR-2 (*rcn1-6*), and amiR-3 (*rcn1-6*), were selected for further analysis. The qRT-PCR analysis data indicated that all three transgenic plants contained *AtPTPA* transcripts that were only 10% or less of the levels found in wild-type and *rcn1-6* mutant plants (Supplemental Fig. S3A). The immunoblot analysis data confirmed that amiR-1 (*rcn1-6*) and amiR-2 (*rcn1-6*) plants contained very low levels of AtPTPA in comparison with the levels found in *rcn1-6* mutant plants (Supplemental Fig. S3B). Like wild-type amiR plants, all amiR (*rcn1-6*) plants were reduced in size relative to *rcn1-6* plants (Supplemental Fig. S4).

In the ABA germination inhibition test, amiR (*rcn1-6*) seeds displayed germination rates of 20% to 40% after 7 d of growth on medium containing 1 μM ABA (Fig. 5A;
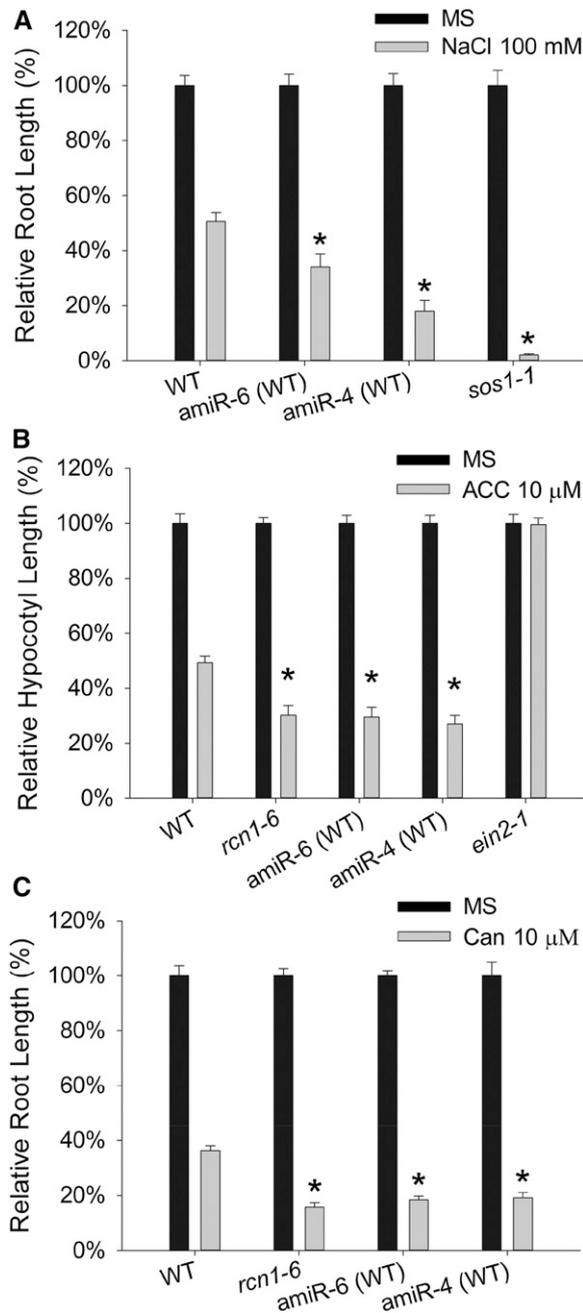
Figure 4. The amiR plants are more sensitive to salt, ethylene, and cantharidin treatments than wild-type plants. A, Relative root lengths of wild-type (WT), *sos1-1* mutant, and two amiR plants in the wild-type background in the absence or presence of 100 mM NaCl. B, Relative hypocotyl lengths of wild-type, *rcn1-6* mutant, amiR-4 (WT), amiR-6 (WT), and *ein2-1* mutant plants in the absence or presence of 10 μM ACC. Plants were grown in darkness for 6 d before measurement. The mutant *rcn1-6* was used as a negative control, and the mutant *ein2-1* was used as a positive control. C, Relative root lengths of wild-type, *rcn1-6* mutant, amiR-4 (WT), and amiR-6 (WT) plants in the absence or presence of the PP2A inhibitor cantharidin (Can; 10 μM). The mutant *rcn1-6* was used as a negative control. Error bars represent SD (*n* = 3). Asterisks indicate *P* < 0.01, as determined by Student's *t* test.

Supplemental Fig. S5A), substantially lower than wild-type amiR seeds (55%–80%; Fig. 3A). Under these conditions, germination of wild-type and *rcn1-6* seeds was 100%. It is not clear why *rcn1-6* seeds are ABA insensitive, but the ABA-insensitive phenotype of *rcn1-6* could be reversed by reduced expression of *AtPTPA*. The germination of amiR (*rcn1-6*) seeds was almost completely inhibited in the presence of 100 mM NaCl (Fig. 5A; Supplemental Fig. S5B). Wild-type and *rcn1-6* seeds were able to germinate after 1 d and turned green after 3 d in the presence of 100 mM NaCl, whereas the amiR (*rcn1-6*) seeds could not germinate even after 5 d. The growth of amiR (*rcn1-6*) seedlings was also more inhibited by cantharidin treatment than that of wild-type plants (Fig. 5A). In the root-bending assay, the root length in amiR (*rcn1-6*) plants was more inhibited than those of wild-type and *rcn1-6* plants even without NaCl treatment, and root growth was completely stopped in amiR (*rcn1-6*) plants exposed to 100 mM NaCl (Fig. 5, B and C). Similarly, hypocotyl length was more strongly reduced in amiR (*rcn1-6*) plants in comparison with wild-type and *rcn1-6* plants that were kept in darkness for 6 d (Fig. 5D). In the presence of ACC, the hypocotyl lengths of amiR (*rcn1-6*) plants were further reduced in comparison with their length under normal conditions (Fig. 5D). These data indicate that reduced expression of *AtPTPA* in the *rcn1-6* background further increases plant sensitivity to ABA, salt, and ethylene, suggesting that reducing the expression of *AtPTPA* in the *rcn1-6* mutant further reduces PP2A activity.

PP2A Activity Was Reduced in amiR Plants

Based on the phenotypes displayed by amiR plants, it is possible that *AtPTPA* deficiency leads to PP2A-deficient phenotypes. To directly test if AtPTPA influences PP2A activity, we determined PP2A activity in cellular extracts prepared from plants of different genetic backgrounds. The results showed that reduction of *AtPTPA* transcript by 90% in wild-type plants [lines amiR-6 (WT) and amiR-4 (WT) in Supplemental Fig. S2] resulted in decreased PP2A activities to about 50% to 60% of the level in wild-type plants. This reduction in PP2A activity was similar to or somewhat greater than that associated with the PP2A mutant *rcn1-6* (Fig. 6). Reduced expression of *AtPTPA* in the *rcn1-6* mutant background [lines amiR-1 (*rcn1-6*) and amiR-2 (*rcn1-6*)] further reduced PP2A activities to about 30% of the wild-type level. The lowest PP2A activity was found in the *rcn1-6* mutant that was treated with 10 μM cantharidin, which was even lower than that found in the PP2A double mutant *a1a2* (Fig. 6). These results clearly indicate that AtPTPA is required for full PP2A activity in Arabidopsis.

It was reported that ABI5, a transcriptional factor that was negatively regulated by PP2A, could be detected at both seed and seedling stages (Lopez-Molina et al., 2001; Liu and Stone, 2010; Hu et al., 2014). Therefore, we measured the transcript of *ABI5* and several *ABI5*-regulated
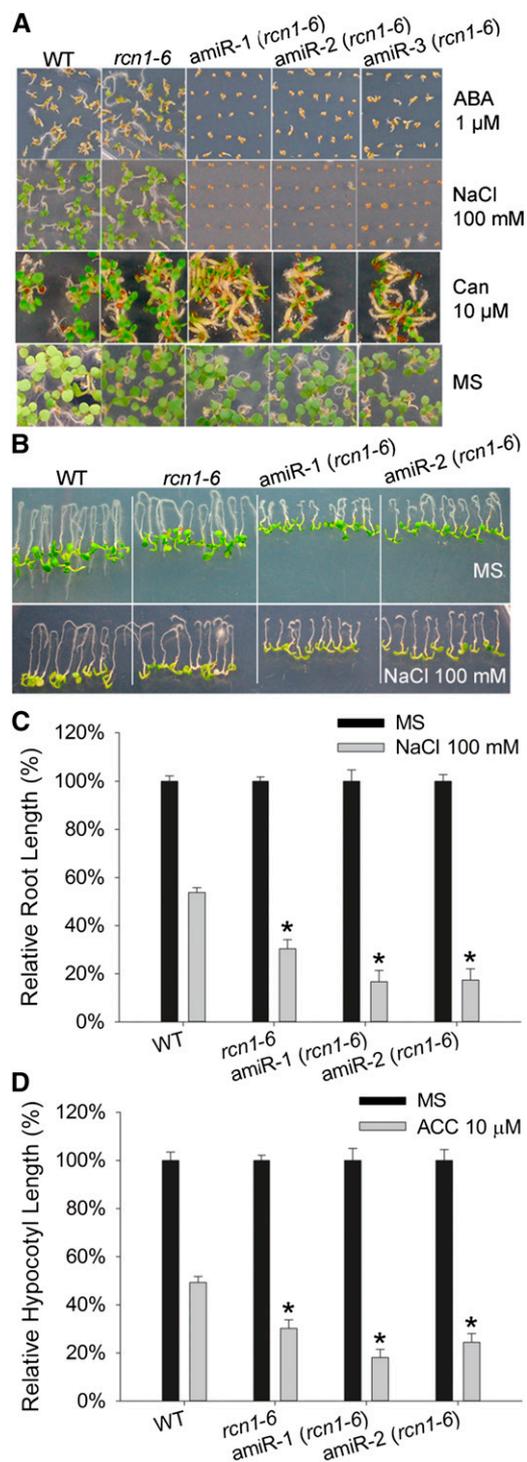
genes at both stages in wild-type and amiR plants. The *ABI5* transcript levels were similar in both wild-type and amiR plants in the presence or absence of ABA (Supplemental Fig. S6, A and E). However, the three *ABI5* downstream genes, *Responsive to dessication 29A* (*RD29A*), *RD29B*, and *Nine-cis-epoxycarotenoid dioxygenase3* (*NCED3*; Finkelstein and Lynch, 2000), were expressed at higher levels in amiR plants when compared with those in wild-type plants after ABA treatment at the seedling stage (Supplemental Fig. S6, B–D). For *ABI5*-regulated genes that were expressed in seed, *RD29A*, *RD29B*, and *Arabidopsis thaliana late embryogenesis abundant1* (*AtEM1*; Finkelstein and Lynch, 2000) were expressed at higher levels in amiR plants when compared with the level found in wild-type plants after ABA treatment (Supplemental Fig. S6, F–H). These results showed that while the expression of *ABI5* transcripts was not affected in amiR plants, *ABI5*-regulated gene expression was increased. Since PP2A negatively regulates ABI5 activity (Hu et al., 2014), these results could be interpreted to indicate that reduced PP2A activity in amiR plants may be responsible for the increased expression of *ABI5* downstream genes.

AtPTPA Is Required for PP2Ac Methylation

To understand how AtPTPA affects PP2A activity in plants, we analyzed the effects of *AtPTPA* deficiency on PP2A assembly and PP2A subunit modification. Research in yeast and human systems suggests that PTPA could change PP2A-C subunit conformation during PP2A assembly (Fellner et al., 2003; Jordens et al., 2006). The change in C subunit conformation could be a prerequisite for PP2A assembly or for C subunit modification. Methylation on Leu-309 of PP2Ac is considered to be essential for PP2A activation in eukaryotic cells (Bryant et al., 1999; Wu et al., 2011). In Arabidopsis, *SBI1* encodes the enzyme responsible for methylating PP2Ac, and it is also required for brassinosteroid signaling (Wu et al., 2011). Therefore, we analyzed the methylation status of PP2Ac in amiR plants.

A putative PP2Ac methylation mutant, *sbi1-2* (Salk_079466), which has a T-DNA insertion into exon 4 of the *SBI1* gene, was obtained from the Arabidopsis Biological Resource Center (ABRC) at Ohio State University. This mutant was characterized to ensure that SBI1 is the key methylating enzyme for PP2Ac in Arabidopsis. Genotyping PCR and semiquantitative

Figure 5. Reduced expression of *AtPTPA* in the *rcn1-6* background by the amiRNA technique leads to more sensitive phenotypes to ABA, NaCl, cantharidin, and ACC treatments. A, Phenotypes of wild-type (WT), *rcn1-6* mutant, and three independent amiR plants in the *rcn1-6* background, amiR-1 (*rcn1-6*), amiR-2 (*rcn1-6*), and amiR-3 (*rcn1-6*), in the absence (MS) or presence of ABA, NaCl, and cantharidin (Can), respectively. Measurements were taken 7 d after plants were moved to MS plates supplemented without or with ABA (1 μM), NaCl (100 mM), or cantharidin (10 μM). B, Phenotypes of wild-type, *rcn1-6* mutant, amiR-1 (*rcn1-6*), and amiR-2 (*rcn1-6*) plants in the absence or presence

of NaCl (100 mM). Photographs were taken 3 d after 4-d-old seedlings were transferred to MS plates without or with NaCl. C, Relative root lengths of wild-type, *rcn1-6* mutant, amiR-1 (*rcn1-6*), and amiR-2 (*rcn1-6*) plants shown in B in the absence or presence of NaCl. D, Relative hypocotyl lengths of wild-type, *rcn1-6* mutant, amiR-1 (*rcn1-6*), and amiR-2 (*rcn1-6*) plants in the absence or presence of ACC. The measurements were taken 6 d after stratified seeds were moved to room temperature in darkness with or without 10 μM ACC. Error bars represent SD ($n = 3$). Asterisks indicate $P < 0.01$, as determined by Student's *t* test.
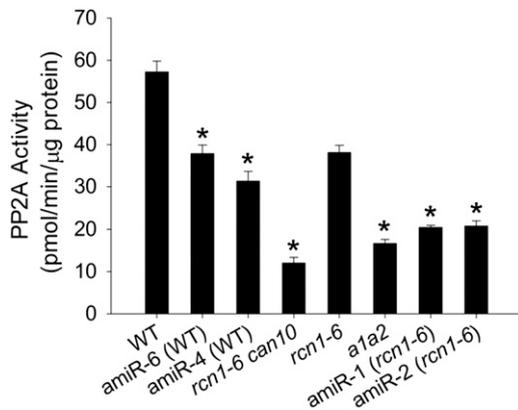
Figure 6. Analysis of PP2A activity in wild-type, PP2A mutants, and amiR plants. WT, The wild type; amiR-6 (WT) and amiR-4 (WT), two independent amiR plants in the wild-type background; rcn1-6, pp2a-a1 mutant; rcn1-6 can10, pp2a-a1 mutant grown on MS plates containing cantharidin (10 μM); a1a2, pp2a-a1/pp2a-a2 double mutant; amiR-1 (rcn1-6) and amiR-2 (rcn1-6), two independent amiR plants in the rcn1-6 mutant background. PP2A activity, defined as pmol phosphate released per min per μg total proteins, was measured with plant materials grown on MS medium for 6 d. Error bars represent sd ($n = 3$). Asterisks indicate $P < 0.01$, as determined by Student's t test.

reverse transcription-PCR experiments confirmed that sbi1-2 is indeed a null allele of the SBI1 gene (Fig. 7, A and B). The PP2A enzymatic assay indicated that PP2A activity in sbi1-2 was significantly reduced relative to that in wild-type plants, to a level similar to the PP2A activity found in rcn1-6 mutant plants (Fig. 7C). Thus, it appears that methylation in PP2Ac is required for full PP2A activity. However, reduction in the expression of AtPTPA led to lower PP2A activity than that found in sbi1-2 and rcn1-6 mutants (Fig. 7C). To confirm the relationship between PP2Ac methylation and PP2A activity, the methylation status of PP2Ac was analyzed in the wild type, sbi1-2, and two wild-type amiR plant lines. As expected, there was a complete loss of PP2Ac methylation in the sbi1-2 mutant (Fig. 7D). We also found significantly reduced PP2Ac methylation in both amiR-4 (WT) and amiR-6 (WT) plants (Fig. 7D). While some residual methylated PP2Ac was detected in extracts from amiR plants, this could be due to residual 10% AtPTPA transcripts found in amiR plants (Supplemental Fig. S2). Because the steady-state levels of the total PP2Ac in amiR plants remained unchanged compared with those in wild-type plants, it appears that AtPTPA deficiency primarily affects PP2Ac methylation.

Reduced PP2Ac Methylation Affects Plant Response to ABA, NaCl, Cantharidin, and ACC

To examine if the loss of methylation in PP2Ac was the reason for the altered responses to hormone and salt stress in amiR plants, the response of the sbi1-2 mutant to ABA, NaCl, cantharidin, and ACC treatments

was studied. Under normal growth conditions, sbi1-2 mutant plants grew normally without apparent developmental defects when compared with wild-type plants (Supplemental Fig. S4). A similar phenotype was reported for the sbi1-1 allele (Wu et al., 2011). However, in response to 10 μM ABA or 100 mM NaCl treatment, the reduction in relative root length in the sbi1-2 mutant was greater than
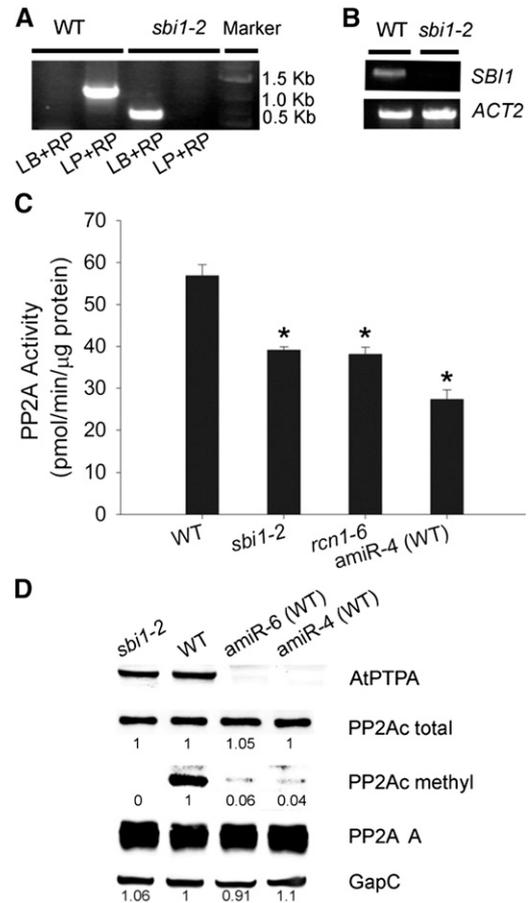

Figure 7. Characterization of the sbi1-2 mutant and immunoblot analysis for total and methylated PP2A-C subunits. A, Confirmation of the sbi1-2 mutant. Genotyping PCR was used to verify the homozygosity of the sbi1-2 mutant. LB, LP, and RP are three primers used in PCR experiments. The LP+RP combination was used to amplify the endogenous genomic SBI1 DNA fragment, whereas the LB+RP combination was used to amplify a partial T-DNA sequence and a partial SBI1 sequence in the T-DNA insertion mutant sbi1-2. B, Reverse transcription-PCR experiment to verify that sbi1-2 is a null mutant. ACTIN2 (ACT2) was used as the internal control. C, Analysis of PP2A activity in wild-type (WT), sbi1-2 mutant, rcn1-6 mutant, and amiR-4 (WT) plants. Plants were grown on MS medium for 6 d before samples were harvested for PP2A enzyme activity assay. Error bars represent sd ($n = 3$). Asterisks indicate $P < 0.01$, as determined by Student's t test. D, Immunoblot analyses of steady-state levels of AtPTPA, total PP2Ac, methylated PP2Ac, and PP2A-A subunits in sbi1-2 mutant, wild-type, and amiR plants. Cytosolic glyceraldehyde-3-phosphate dehydrogenase (GapC) was used as the protein loading control. The relative abundance (compared with the wild type) for total PP2Ac, methylated PP2Ac, and cytosolic glyceraldehyde-3-phosphate dehydrogenase is shown below each band.

that in wild-type plants (Fig. 8A). Similar results were obtained when plants were treated with 10 μM cantharidin or 10 μM ACC (Fig. 8, B and C). Although somewhat less severe, the response of *sbi1-2* plants under these conditions was similar to that of amiR-4 (WT) and amiR-6 (WT) plants. While these results indicate that lack of PP2Ac methylation alone may not be fully responsible for all phenotypes observed in amiR plants, nevertheless, reduced PP2Ac methylation in amiR plants is likely a substantial contributing factor to their altered responses to ABA, salt, and ACC.

AtPTPA Interacts with Both A and C Subunits

AtPTPA deficiency leads to reduced PP2Ac methylation, suggesting that AtPTPA either affects PP2A assembly or PP2A subunit structures. To test these possibilities, immunoprecipitation experiments were first performed. Transgenic plants that express a GFP-AtPTPA fusion protein were created (Supplemental Fig. S7) for the analysis to determine if AtPTPA and PP2A interact with each other in vivo. PP2A-A antibodies were used to immunoselect A subunit-interacting proteins from cellular extracts of wild-type, *rcn1-6*, RCN1-yellow fluorescent protein (YFP; Blakeslee et al., 2008), and GFP-AtPTPA plants. AtPTPA- and PP2Ac-specific antibodies were then used in the immunoblot experiments. As expected, PP2A-A antibodies could immunoselect both AtPTPA and C subunits (Fig. 9A). In a reciprocal experiment, a glutathione *S*-transferase (GST)-AtPTPA fusion protein was used to immunoselect AtPTPA-interacting proteins from cellular extracts of wild-type and amiR-4 (WT) plants. While both A and C subunits were immunoselected in these assays, more C subunits were immunoselected in amiR-4 (WT) plants than in wild-type plants (Fig. 9B). Only a small amount of PP2A-C subunits was detected, which agreed with earlier reports that the interaction between PTPA and PP2A-C is weak (Fellner et al., 2003).

PP2Ac Methylation and AtPTPA-PP2Ac Interaction Are Both A Subunit Dependent

Since free PP2Ac has been shown to have much higher activities against nonspecific substrates that could have toxic effects on cells (Fellner et al., 2003; Hombauer et al., 2007), PP2A-C subunits in eukaryotic cells usually interact with regulatory proteins that increase their specificity. For example, A subunits are generally required to control the nonspecific activity of PP2As (Ruediger et al., 1992; Hombauer et al., 2007). Therefore, we investigated whether, like AtPTPA, A subunits are required for PP2Ac methylation. To address this question, the methylation status of PP2Ac in the wild type, *a1* mutant (*rcn1-6*), *a2a3* double mutant, and *a1a2* double mutant was analyzed. A1 is the most important A subunit in PP2A (Zhou et al., 2004), and its loss in the *rcn1-6* mutant leads to a 50% reduction in
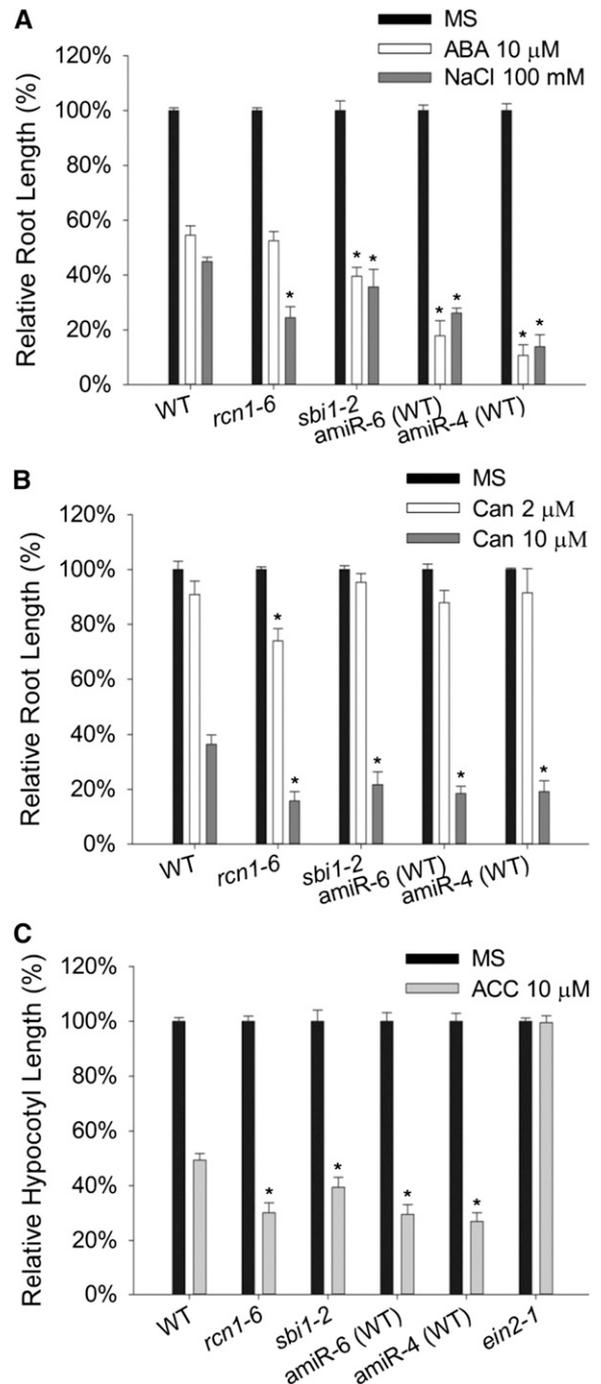

Figure 8. Phenotypes of wild-type, *rcn1-6* mutant, *sbi1-2* mutant, and amiR plants after treatments with ABA, NaCl, cantharidin, and ACC. A, Relative root lengths (%) of wild-type (WT), *rcn1-6* mutant, *sbi1-2* mutant, and two amiR plants after treatments with ABA (10 μM) or NaCl (100 mM). Four-day-old seedlings were transferred to MS plates containing no ABA or NaCl or containing ABA or NaCl for 3 d before root length was measured. B, Relative root lengths on MS plates containing no cantharidin or MS plates containing cantharidin (Can; 2 and 10 μM) for 3 d before root length was measured. C, Relative hypocotyl lengths on MS plates containing no ACC or MS plates containing ACC (10 μM) for 3 d before root length was measured. The ethylene-insensitive mutant *ein2-1* was used as a positive control for this assay. Error bars represent SD ($n = 3$). Asterisks indicate $P < 0.01$, as determined by Student's *t* test.
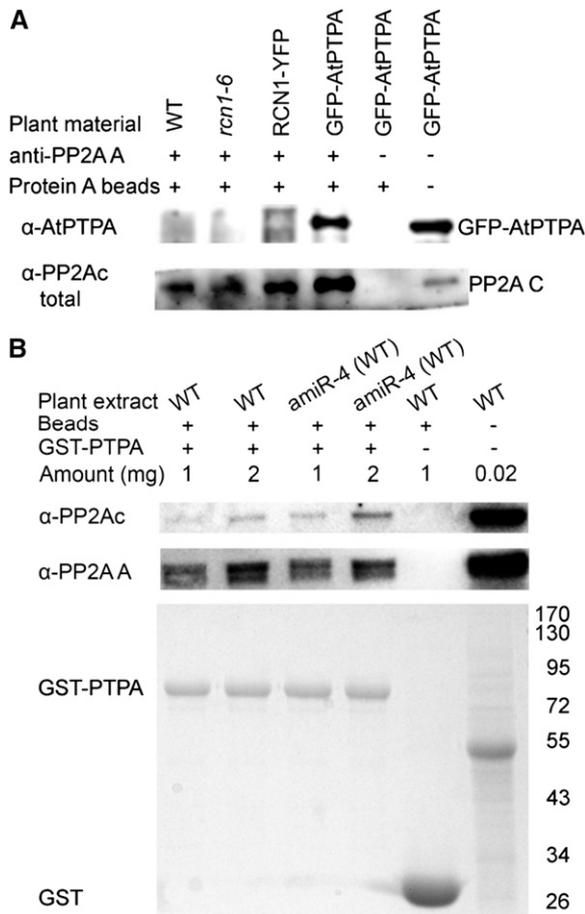
Figure 9. AtPTPA interacts with PP2A-A and PP2A-C subunits. A, Immunoprecipitation experiments to demonstrate that PP2A-A subunits interact with AtPTPA and PP2A-C subunits. PP2A-A antibodies were used as the pulling antibodies, and AtPTPA antibodies and PP2Ac antibodies were used in the western-blot experiments. Plant cellular extracts were from the wild type (WT), the *rcn1-6* mutant, *RCN1-YFP*-overexpressing plants in the *rcn1-1* background, and *GFP-AtPTPA*-overexpressing plants. Extracts from *GFP-AtPTPA*-overexpressing plants, but no pulling antibodies, were used as the negative control. Extracts from *GFP-AtPTPA*-overexpressing plants were loaded directly for the positive control on the blot. B, Pull-down experiments to demonstrate that GST-AtPTPA interacts with PP2A-C and PP2A-A subunits. Glutathione-agarose beads were used as the pulling matrix, and PP2Ac and PP2A-A antibodies were used in the western-blot experiments. Cellular extracts from wild-type and amiR-4 (WT) plants were used in pull-down experiments. GST alone was used as a negative control for the pull-down experiments, and extracts from the wild type were loaded directly in the western-blot experiment. Coomassie Brilliant Blue staining of pull-down mixtures is shown below.

the methylation of PP2Ac (Fig. 10A). A further loss in the A2 subunit in the *a1a2* background resulted in reduction in PP2Ac methylation by 90%, a clear indication that A subunits are required for PP2Ac methylation. Recent work by Stanevich et al. (2014) explored the structural requirement of A subunits in the process of methylating PP2Ac, corroborating our results that A subunits are essential for PP2Ac methylation.

Interestingly, the total levels of C subunits in plant cell extracts were not as much affected in *a1a2* double mutant seedlings, indicating that, in addition to A subunits, other factors may be involved in binding C subunits. Furthermore, although AtPTPA is required for PP2Ac methylation, its deficiency in amiR plants does not affect the abundance of C subunits in plant cells (Fig. 7D). When PP2A-A antibodies were used to pull down C subunits from extracts of various genetic backgrounds, we found that the amount of C subunits bound to A subunits was not much different among wild-type, *sbi1-2*, amiR-4 (WT), and amiR-6 (WT) plants (Fig. 10B), indicating that the methylation status of PP2Ac does not affect the binding of PP2Ac to A subunits. In addition, when pull-down experiments were performed with cellular extracts from the *pp2a* mutants, *rcn1-6*, and $a1^{-/-}a2^{+/-}$, less C subunit was coselected with AtPTPA than from wild-type cellular extracts (Fig. 10C), the opposite of what was observed when cellular extracts of wild-type amiR plants (Fig. 9B) were used. However, the steady level of PP2Ac in the *rcn1-6* mutant is similar to the PP2Ac level in wild-type plants (Fig. 10A), indicating that AtPTPA may specifically bind to AC dimers, not to free PP2Ac. These data also hint at the existence of a PP2A-A/AtPTPA/PP2Ac complex in Arabidopsis.

AtPTPA Deficiency Reduces the Binding of B Subunits to C Subunits

To examine the *AtPTPA* deficiency on PP2A holoenzyme assembly, protein-protein interactions between B subunits and C subunits were studied using immunoselection experiments. We found that the B subunits ATB' η (At3g26020) and ATB' γ (At4g15415) could bind to PP2Ac in cellular extracts from all genetic backgrounds (Fig. 11). However, substantial differences in their binding efficiency to C subunits were seen. While substantial amounts of C subunit were coselected with the ATB' η B subunit from extracts of wild-type plants, very little was recovered from extracts of the *sbi1-2* plants (Fig. 11A). The amount of C subunit immunoselected by ATB' η from *rcn1-6* mutant and amiR-4 (WT) plant extracts was reduced relative to that from wild-type plants but greater than that from the *sbi1-2* mutant. Comparison of the interaction of ATB' η in extracts from wild-type plants, in which most C subunits are methylated, and *sbi1-2* mutant plants, which contain only unmethylated C subunits, indicates that binding of ATB' η to unmethylated C subunits is very inefficient. Since both AtPTPA and A subunits are required for PP2Ac methylation (Figs. 7 and 10), reduced methylation could explain why less C subunit is immunoselected by ATB' η in the *rcn1-6* mutant and amiR-4 (WT) plants (Fig. 11A).

The binding of ATB' γ to PP2Ac shows different characteristics. Similar amounts of PP2Ac were coselected from cellular extracts of *sbi1-2* and wild-type plants (Fig. 11B), indicating that this B subunit binds efficiently
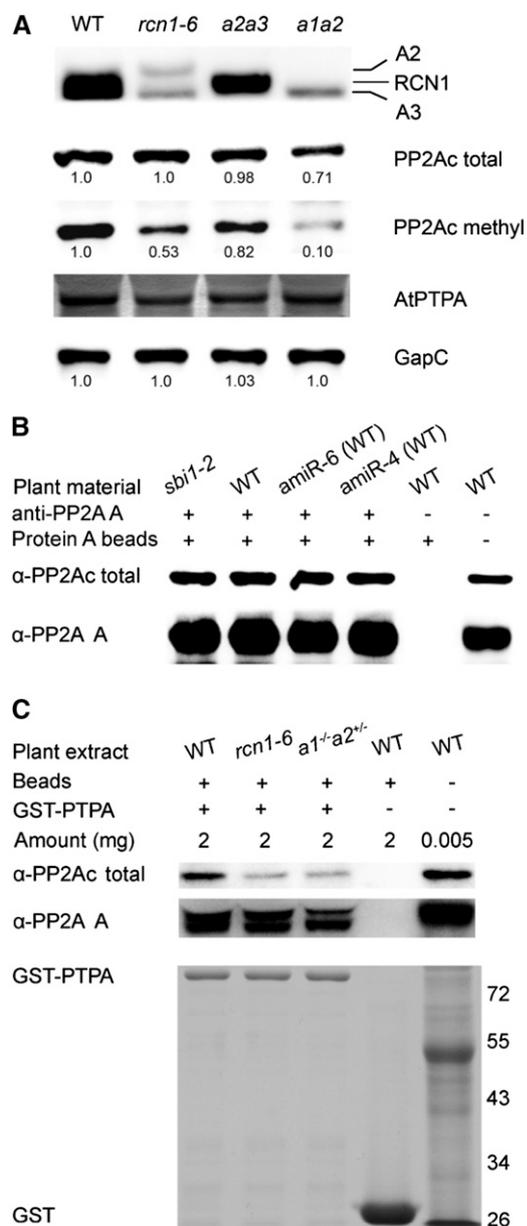
Figure 10. Methylation of PP2A-C subunits is dependent on PP2A-A subunits, and the protein-protein interaction between AtPTPA and PP2A-C subunits is PP2A-A dependent. A, Western-blot analyses of PP2A-A subunits, PP2Ac, methylated PP2Ac, and AtPTPA in the wild type (WT), *pp2a-a1* mutant (i.e. *rcn1-6*), *pp2a-a2/pp2a-a3* double mutant (*a2a3*), and *pp2a-a1/pp2a-a2* double mutant (*a1a2*). Cytosolic glyceraldehyde-3-phosphate dehydrogenase (GapC) was used as the protein loading control. The relative abundance (compared with the wild type) for total PP2Ac, methylated PP2Ac, and cytosolic glyceraldehyde-3-phosphate dehydrogenase is shown below each band. B, Immunoprecipitation analysis of protein-protein interaction between PP2A-A subunit and PP2Ac. PP2A-A antibodies were used as the pulling antibodies, and PP2Ac antibodies were used in the western-blot experiment. Plant cellular extracts were from *sbi1-2*, wild-type, amiR-6 (WT), and amiR-4 (WT) plants in the immunoprecipitation experiment and cellular extracts (20 µg of proteins) from wild-type plants were loaded directly in the western-blot experiment. C, Pull-down experiments to show that the interaction

to both methylated and unmethylated C subunits. This result helps to explain why the total loss of PP2Ac methylation in *sbi1-2* mutant plants does not eliminate PP2A activity. This may also explain why the *sbi1-2* mutant appears to be healthy under normal growth conditions. In addition, both B subunits brought down less PP2Ac from amiR plants than from wild-type plants, indicating that *AtPTPA* is required for the interaction between B and C subunits.

DISCUSSION

This study provides evidence that the PTPA ortholog in Arabidopsis, AtPTPA, plays an essential role in plant growth and development. First, *AtPTPA* is expressed in most tissues analyzed, especially in flower, stem, and roots (Fig. 1), suggesting that AtPTPA is likely required for cellular metabolism in these tissues. Next, the reduction of *AtPTPA* expression using the amiRNA technique caused pleiotropic phenotypic characteristics in transgenic plants, including smaller plant size and altered responses to ABA, NaCl, ACC, and cantharidin (Figs. 2–5). Reduced PP2A activity in the *pp2a-c2* mutant led to similar responses to NaCl treatments (Pernas et al., 2007), and reduced PP2A activity in *rcn1-6* mutant also led to similar responses to NaCl, ACC, and cantharidin treatments (Larsen and Chang, 2001; Kwak et al., 2002; Muday et al., 2006), indicating a causal relationship between reduced PP2A activity and increased sensitivity to NaCl, ACC, and cantharidin treatments. The amiR plants created in this study also had reduced PP2A activity (Fig. 6), indicating that, like PTPA in human cells or RRD1 and RRD2 in yeast, AtPTPA is directly involved in the regulation of PP2A activity in Arabidopsis. More specifically, the results presented here indicate that AtPTPA is required for PP2Ac methylation (Fig. 7), and loss of PP2Ac methylation in the *sbi1-2* mutant led to similar phenotypes to those found in amiR plants (Fig. 8). However, the *sbi1-2* mutant shows less severe phenotypes than wild-type amiR plants, suggesting that *AtPTPA* functions upstream of *SBI1*. Furthermore, immunoselection assays showed that AtPTPA could bring down both A and C subunits (Fig. 9B), and the binding between AtPTPA and PP2Ac is A subunit dependent (Fig. 10C). Further immunoselection assays demonstrate that A subunits are also required for PP2Ac methylation (Fig. 10A). Finally, we found that individual B subunits have different

between AtPTPA and PP2A-C subunits is PP2A-A dependent. Glutathione-agarose beads were used as the pulling matrix, and PP2Ac and PP2A-A antibodies were used in the western-blot experiments. Cellular extracts from wild-type, *pp2a-a1* mutant (*rcn1-6*), and *pp2a-a1 pp2a-a1/PP2A-A2 pp2a-a2* mutant (*a1⁻/⁻ a2⁺/⁻*) plants were used in pull-down experiments. GST alone was used as a negative control for the pull-down experiments, and extracts from the wild type were loaded directly in western-blot experiments. Coomassie Brilliant Blue staining of pull-down mixtures is shown below.
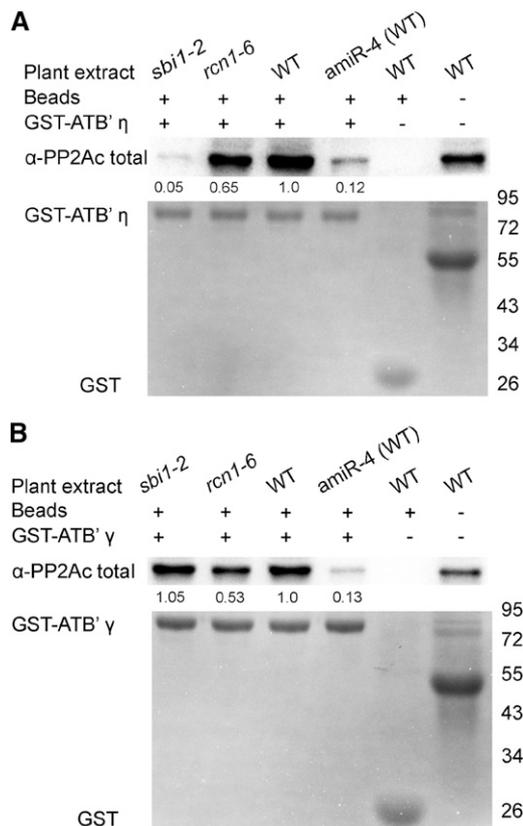
Figure 11. Pull-down experiments to show differential binding of PP2A-B subunits to PP2Ac. A, The PP2A-B subunit ATB′ η preferentially binds to methylated PP2Ac. B, The PP2A-B subunit ATB′ γ binds to both methylated and unmethylated PP2Ac. Cellular extracts from *sbi1-2*, *rcn1-6*, wild-type (WT), and amiR-4 (WT) plants were used in the pull-down experiments, and PP2Ac antibody was used in the western-blot experiment. Cellular extracts from the wild type were loaded in the western-blot analysis. Coomassie Brilliant Blue staining of pull-down mixtures is shown below. The relative abundance (compared with the wild type) for total PP2Ac is shown below each band.

affinities for methylated and unmethylated PP2Ac. The ATB′ η subunit appears to bind specifically with methylated PP2Ac, while binding of the ATB′ γ subunit appears to be methylation independent (Fig. 11). The interactions between these two B subunits and PP2Ac were much weaker in extracts from amiR plants than from wild-type plants, indicating that AtPTPA is required for B and C interaction in the process of holoenzyme formation.

Based on these data, we propose that AtPTPA functions as a critical regulator that controls PP2A holoenzyme assembly (Fig. 12). In this capacity, AtPTPA changes the conformation of the C subunit in the AC dimer so that the C subunit can interact with a B subunit to form a trimeric holoenzyme or allow the C subunit to be methylated by SBI1 before being assembled into a trimeric holoenzyme (Fig. 12). The strength of enzyme activity of the PP2A holoenzyme formed could depend on whether the C subunit is methylated by SBI1. AtPTPA participates in the PP2A assembly process after

the AC dimer is already formed, since AtPTPA deficiency does not affect the interactions between A and C subunits (Fig. 10B). In yeast, RRD1/RRD2 can bind to inactive C subunits and promote PP2A holoenzyme assembly (Fellner et al., 2003; Hombauer et al., 2007). Our immunoselection experiments also detected protein-protein interaction between AtPTPA and C subunits. Interestingly, AtPTPA showed the strongest PP2Ac precipitation from cellular extracts of amiR-4 (WT) plants (Fig. 9B) and the weakest from cellular extracts of the *pp2a-a1* mutant (Fig. 10C). We hypothesize that, because the binding of PTPA to PP2Ac is A subunit dependent, fewer C subunits are associated with A subunits in the *pp2a-a1* mutant; therefore, less PP2Ac was precipitated in the cellular extracts of *rcn1-6* or $a1^{-/-}a2^{+/-}$ mutants (Fig. 10C). In amiR-4 (WT) plants, more PP2Ac is associated with A subunits that could not be assembled into PP2A holoenzyme; therefore, more PP2Ac was precipitated by AtPTPA compared with extracts from wild-type plants. Our immuno-selection experiments with B subunits, ATB′ η and ATB′ γ, show that the interactions between B subunits and C subunits are AtPTPA dependent, and less functional PP2Ac is available in amiR plants (Fig. 11). This model suggests that there is an intermediate complex, PP2A-A/PP2A-C/AtPTPA, between an AC dimer whose phosphatase activity is unknown and the AC dimer that is committed to become a PP2A holoenzyme (Fig. 12). The final PP2A enzyme formed, however, could have higher or lower PP2A activities, depending on whether or not the C subunit is methylated.

Free PP2A-C subunits could pose serious risks to cellular metabolism, since they possess high, promiscuous activities in vitro (Mumby et al., 1985; Tung et al., 1985). Thus, C subunits are usually associated with a regulatory protein such as PP2A-A subunit (Ruediger et al., 1992) or 2A phosphatase-associated protein of 46 KD (Hu et al., 2014) to prevent such potential toxic activity. AtPTPA

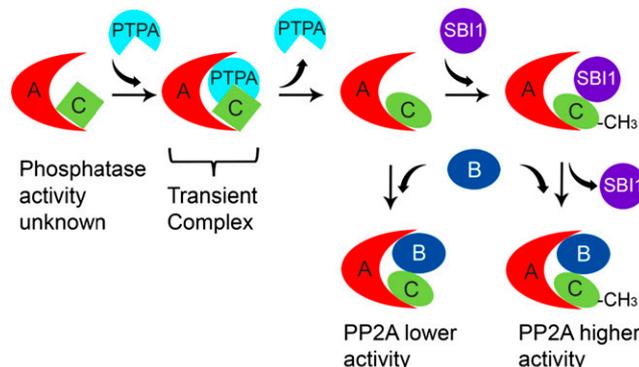**Figure 12.** Model of the function of AtPTPA in the assembly of the PP2A holoenzyme in plants. AtPTPA, together with an A subunit of PP2A, binds to a PP2A-C subunit and converts it into a form that can accept a B subunit or be methylated by SBI1 before accepting a B subunit. The PP2A holoenzyme containing a methylated C subunit is more active (higher activity) than the one with a C subunit without methylation (lower activity).

appears to be a critical regulator that commits the AC dimer to the formation of a PP2A holoenzyme. Therefore, regulation of *AtPTPA* expression could determine where and how much PP2A holoenzyme can be formed. Reduced expression of *AtPTPA* leads to severe defects in plant development and plant responses to ABA, ethylene, and salt. It is not clear why *rcn1-6* plants display an ABA-insensitive phenotype. Kwak et al. (2002) proposed that RCN1 might serve as a general transducer at the early ABA signaling pathway and that the *rcn1-6* mutation impaired ABA-induced stomata closing. RCN1 also may interact with unknown proteins that function upstream of PP2A in ABA signaling, as *AtPTPA* deficiency reduced PP2A activity and reversed the ABA-insensitive phenotype of the *rcn1-6* mutant (Fig. 5A). Nevertheless, like the *pp2a-c2* mutant, *rcn1-6* mutant plants also have reduced PP2A activity and increased sensitivity to salt (Pernas et al., 2007). Taken together, these data indicate that AtPTPA is an important factor in the assembly of the fully functional PP2A holoenzyme.

PP2Ac methylation is common among eukaryotes, and approximately 50% to 90% of PP2A-C subunits are found to be methylated in eukaryotic cells. Demethylated PP2A-C subunits were shown to be less competent for binding to some regulatory B subunits (Wu et al., 2000). In plants, more than 80% of PP2Ac is methylated to ensure high specific activity for particular substrates (Wu et al., 2011). The *sbi1-1* mutant is completely devoid of methylated PP2Ac, yet the mutant is relatively healthy under normal conditions (Wu et al., 2011). In the knockout mutant *sbi1-2*, total PP2A activity drops by 30% (Fig. 7C), indicating that PP2Ac methylation affects PP2A activity. Furthermore, PP2Ac methylation affects its subcellular localization and terminates activated brassinosteroid signaling (Wu et al., 2011), indicating that PP2Ac methylation also plays a role in the signaling pathway of this plant hormone. On the other hand, *a1a2* double mutant plants had significantly less methylated PP2Ac and reduced levels of total PP2Ac, suggesting that A subunits are not just required for methylating PP2Ac but also are essential for maintaining the steady-state levels of total PP2Ac in plant cells.

The function of AtPTPA goes beyond the methylation of PP2Ac. Its main function is to convert PP2Ac into a form that can accept B subunits. A small fraction of PP2Ac exists in this form in wild-type plants, but it accumulates in *sbi1* mutant plants. There is no methylated PP2Ac in the *sbi1-2* mutant plants, but residual PP2Ac methylation remains in amiR plants. However, *sbi1-2* plants share similar, but less severe, phenotypes in response to hormone and salt treatments when compared with amiR plants. Mutant *sbi1-2* plants had 70% of the total PP2A activity of wild-type plants, while amiR plants had only 50% to 60% of the PP2A activity found in wild-type plants (Fig. 6). In addition, even though *sbi1-2* resembles *rcn1-6* in terms of plant size and fertility, amiR plants display far more severe developmental defects, including dwarf size and reduced fertility. These observations indicate to us that the loss of PP2Ac methylation may not be the sole reason for the reduced PP2A activity in amiR plants. Despite their low abundance, some active PP2As in plants must have C subunits that are not methylated. In *sbi1-2* mutant plants, complete loss of PP2Ac methylation only led to about 30% reduction in PP2A activity, but the total PP2Ac level was unchanged. This supports our assertion that unmethylated PP2Ac is still active in the *sbi1-2* mutant but is likely to be less active than the methylated form. Moreover, amiR plants had a greater reduction of PP2A activity than the *sbi1-2* mutant, supporting the idea that AtPTPA is required for the transformation of PP2Ac into an intermediate form before being assembled into a functional trimeric enzyme, regardless of its final methylation status.

PP2A activity is likely to be controlled by several factors. The first is the abundance of PP2Ac proteins. Overexpression of *PP2A-C2* was shown to increase PP2A activity in transgenic plants by 40% (Pernas et al., 2007). Even though the relationship between activity and protein abundance is not strictly linear, it does suggest that PP2Ac protein abundance is a contributing factor for PP2A activity in vivo. The second factor is the modifications at the C-terminal end of PP2A-C subunits (PP2Ac methylation), as discussed here. The third factor is the abundance of PP2A-A subunits, since loss of the PP2A-A1 subunit (RCN1) leads to the loss of PP2Ac methylation and the steady-state levels of PP2A-C subunits (Fig. 10). The fourth factor, and perhaps the most important one, is AtPTPA, which is critical in the formation of the AC dimer that can bind to a B subunit to become a trimeric holoenzyme.

MATERIALS AND METHODS

Plant Materials and Growth Conditions

The Arabidopsis (*Arabidopsis thaliana*) T-DNA insertion mutant *rcn1-6* (Blakeslee et al., 2008) and *a1*$^{-/-}$*a2*$^{+/-}$ and *a2a3* mutants (Zhou et al., 2004) were kindly provided by Dr. Alison Delong. The *sos1-1* mutant (Shi et al., 2000) was a kind gift from Dr. Huazhong Shi, and the *ein2-1* mutant (Alonso et al., 1999) and the *sbi1-2* mutant were obtained from the ABRC (stock no. CS3071 and Salk_079466, respectively). Seeds were surface sterilized with 75% (v/v) ethanol for 1 min and then kept in 15% (v/v) bleach for 5 min, followed by rinsing in sterilized distilled water for 5 min. After being kept in the dark at 4°C for 3 d, seeds were transferred onto 0.5× MS medium (0.8% [w/v] agar, 0.5× MS salts, 1% [w/v] Suc, and 0.5 g L^{-1} MES, pH 5.7) and grown under constant light at room temperature.

Construction of Transforming Vectors and Arabidopsis Transformation

For P$_{AtPTPA}$::*GUS* transgenic plants, a 1.7-kb fragment of *AtPTPA*'s 5′ sequence was PCR amplified with the primers proPTPA-F1 and proPTPA-R1 (Supplemental Table S1), digested with *Hin*dIII and *Bam*HI, and then cloned into the binary vector pBI121 (Jefferson et al., 1987) to replace the cauliflower mosaic virus 35S promoter using the same *Hin*dIII/*Bam*HI sites. Wild-type Arabidopsis plants were transformed with the vector made above by using the floral dip transformation method (Clough and Bent, 1998). Primary transgenic plants were selected on 0.5× MS medium containing 30 μg mL^{-1} kanamycin, and 30 independent transgenic plants were obtained. Eight single-copy T-DNA insertion lines were selected for further propagation until homozygous lines were obtained at the T3 generation before proceeding to histochemical staining analyses.

To create amiR plants, an amiRNA was created using the primers amiR-I, amiR-II, amiR-III, and amiR-IV (Supplemental Table S1) and then cloned into the binary vector pFGC5941 at the *Asc*I and *Bam*HI sites (the vector was ordered from the ABRC; stock no. CD3-447). The recombinant binary vector was then transformed into *Agrobacterium tumefaciens* strain GV3101 and introduced into wild-type plants through the floral dip transformation method (Clough and Bent, 1998). Putative transformants were selected on 0.5× MS plates containing 50 μg mL^{-1} Basta; 46 independent transgenic plants were obtained, and eight lines with strong phenotypes were selected for further analyses until homozygous lines were obtained after the T3 generation. Then, three selected homozygous lines, amiR-4 (WT), amiR-6 (WT), and amiR-10 (WT), were used for *AtPTPA* transcript analysis using RNA-blot and qRT-PCR techniques. The same amiRNA construct was transformed into the *rcn1-6* mutant, and 30 independent transgenic plants were obtained, among which three homozygous lines that displayed strong phenotypes, amiR-1 (*rcn1-6*), amiR-2 (*rcn1-6*), and amiR-3 (*rcn1-6*), were selected for detailed characterization.

For GFP-AtPTPA transgenic plants, a cDNA fragment coding for a full-length *AtPTPA* was amplified with primers ox-PTPA-F and ox-PTPA-R and then cloned into the pBI121-GFP intermediate vector (Shen et al., 2010) at the *Bam*HI and *Sac*I sites. Wild-type plants were transformed with the floral dip transformation method (Clough and Bent, 1998) using the GFP-AtPTPA vector created, and putative transformants were selected on MS plates containing 30 μg mL^{-1} kanamycin. There were 30 independent transgenic plants obtained, and five high-expression/single-copy T-DNA insertion lines were selected for further analyses.

Histochemical Staining of P_{AtPTPA}::GUS Transgenic Plants

Three-day-old seedlings, 6-d-old seedlings, and other tissues from 5-week-old plants of P_{AtPTPA}::GUS homozygous transgenic lines were submerged into the GUS staining solution [100 mM sodium phosphate, pH 7, 0.1% (v/v) Triton X-100, 10 mM EDTA, 0.5 mM K$_3$Fe(CN)$_6$, 0.5 mM K$_4$Fe(CN)$_6$, and 1 mM 5-bromo-4-chloro-3-indolyl glucuronide] and kept at 37°C for 24 h before removing the chlorophylls with 95% (v/v) ethanol. Images of stained seedlings were taken using a microscope connected to a digital camera, and other images of stained tissues were captured with the Nikon D50 6.1 MP Digital SLR Camera.

Hormone, NaCl, and Cantharidin Treatments

For the seed germination test, seeds were plated in 0.5× MS medium supplemented with different concentrations of ABA (1, 2, and 5 μM). Seeds were counted as germinated based on protrusion of the radicle. For the root elongation test in different hormone or salt stress treatments, 4-d-old seedlings grown on 0.5× MS medium were transferred onto medium supplemented with one of the following compounds: 10 μM ABA, 100 mM NaCl, 2 μM cantharidin, and 10 μM cantharidin. Seedlings were allowed to grow for an additional 3 or 4 d before root length was measured. For the root-bending test on NaCl-containing medium, similar procedures were followed as above, but the seedlings were grown upside down. For the hypocotyl elongation test, seeds were grown on medium supplemented with or without 10 μM ACC. These plants were allowed to grow vertically for 6 d in darkness at room temperature before hypocotyl length was measured.

RNA Isolation, RNA-Blot Analysis, and qRT-PCR Experiments

Plant samples were harvested, immediately frozen in liquid nitrogen, and kept in a −80°C freezer before use. Total RNAs were isolated using the Trizol reagent from Invitrogen according to the manufacturer's protocol. Precipitated RNA samples were dissolved in water, the concentration of total RNAs was measured using Nanodrop-1000 equipment from Thermo Scientific, and all RNA samples were normalized to a concentration of 1 μg μL^{-1} before use. For RNA-blot analysis, 10 μg of total RNAs of each sample was separated on a denatured agarose gel and transferred onto a nylon membrane. The ^{32}P-labeled DNA probes were prepared using a random priming kit (DECAprime II) from Life Sciences according to the manufacturer's protocol with the full-length cDNA of *AtPTPA* and *ACTIN2* as templates. Hybridization and washing conditions were conducted as reported previously (Shen et al., 2010). The results of RNA blots were captured using the Storm 860 Molecular Imager from GE Healthcare. For qRT-PCR, 2 μg of total RNAs was

first reverse transcribed using the SuperScript VILO cDNA Synthesis Kit from Invitrogen according to the manufacturer's protocol. The qRT-PCR and data processing was performed with the Applied Biosystems 7500 Real-Time PCR System. The primers for qRT-PCR analysis of *AtPTPA*, *ABI5*, and the internal control gene *ACTIN8* were PTPA-F and PTPA-R, ABI5-F and ABI5-R, and Actin-F and Actin8-R, respectively. To analyze *ABI5* downstream gene expression in wild-type and amiR plants, the following oligonucleotide pairs were used: AtEM1-F and AtEM1-R, RD29A-F and RD29A-R, RD29B-F and RD29B-R, and NCED3-F and NCED3-R. The sequence information for qRT-PCR is listed in Supplemental Table S1.

Characterization of the *sbi1-2* Mutant

Because the *sbi1-1* mutant is not in the Columbia ecotype, we obtained another *sbi1* mutant from the ABRC that is in the Columbia background. This new T-DNA insertion mutant, with accession number Salk_079466, was named *sbi1-2*. We used oligonucleotide primers LP and RP to amplify the endogenous genomic DNA of *SBI1* from wild-type plants and primers LB and RP to amplify partial T-DNA-specific sequence and partial endogenous genomic DNA of *SBI1* from the *sbi1-2* mutant (Fig. 7A). We used oligonucleotide primers SBI1-RTF and SBI1-RTR to amplify cDNA reverse transcribed from the *SBI1* transcript in both the wild type and the *sbi1-2* mutant (Fig. 7B). The sequence information on oligonucleotide primers is provided in Supplemental Table S1.

Preparation of GST Fusion Proteins and AtPTPA Antibodies

The full-length cDNAs of *AtPTPA*, *ATB′ η*, and *ATB′ γ* were amplified from an Arabidopsis cDNA library with primers GST-PTPA-F1 and GST-PTPA-R1, GST-ATB′ η-F and GST-ATB′ η-R, and GST-ATB′ γ-F and GST-ATB′ γ-R (Supplemental Table S1) and then subcloned into the protein expression vector pGSTag (Ron and Dressler, 1992) to make the recombinant vectors pGST-AtPTPA, pGST-ATB′ η, and pGST-ATB′ γ for protein expression in bacterial cells. The *Escherichia coli* strain BL21 harboring these constructs were grown in Luria-Bertani medium supplemented with 100 μg mL^{-1} ampicillin at 37°C until its density, measured as optical density at 600 nm, reached 0.4. Isopropyl β-D-1-thiogalactopyranoside was then added into the medium to a final concentration of 1 mM for protein induction for 4 h before cells were harvested. Cells were then centrifuged at 5,000g for 10 min and washed three times with phosphate-buffered saline (pH 7.3). Crude protein extracts were obtained through sonication using the Ultrasonic Processor from Cole-Parmer. GST fusion proteins were then purified from crude extracts with glutathione-agarose beads from Sigma according to the manufacturer's protocol. The purified GST-AtPTPA fusion proteins were treated with protease thrombin to release the full-length AtPTPA protein from beads before it was sent to Sangon Biotech for antibody production. The AtPTPA antibodies made by Sangon Biotech could detect a clear band from 5 μg of leaf cellular extracts in western-blot analysis (Supplemental Fig. S8A).

Protein Extraction and Immunoblot Analysis

Plant samples were harvested in liquid nitrogen and kept in a −80°C freezer before use. The samples were first ground into fine powder and then resuspended thoroughly in the extraction buffer (50 mM NaPO$_4$, pH 7, 1 mM EDTA, and 0.1% [v/v] Triton X-100). The crude extracts were then centrifuged at 13,000g for 10 min at 4°C. The supernatants were transferred to a fresh tube. Protein concentration was determined using the method of Bradford (1976).

For immunoblot analysis, 20 μg of total cellular proteins was denatured in 2× SDS loading buffer (62.5 mM Tris-Cl, 1% [w/v] SDS, 10% [v/v] glycerol, 100 mM dithiothreitol [DTT], and 0.01% [w/v] Bromphenol Blue, pH 6.8) and then separated on a 12% SDS (w/v) polyacrylamide gel. Rabbit polyclonal antibodies for AtPTPA and cytosolic glyceraldehyde-3-phosphate dehydrogenase were used to detect their respective antigens in a dilution of 1:2,000. PP2A-A3 antibodies, made in our laboratory (Hu et al., 2014), were used in a dilution of 1:1,500. Both PP2Ac total antibody and PP2Ac methylation-specific antibody were purchased from EMD (catalog nos. 07-324 and 04-1479) and were used in a dilution of 1:1,000. Both commercial antibodies were used previously by Wu et al. (2011) to study the *sbi1-1* mutant. In our hands, these two antibodies could detect PP2Ac from 5 μg of total cellular protein extracts (Supplemental Fig. S8B). The specificity of PP2Ac methylation antibody was also tested using the base washing

method (Wu et al., 2011). Before being washed extensively, the protein blots were first treated with or without NaOH (0.2 N) for 30 min, then probed with PP2Ac methylation antibody and PP2Ac total antibody (Supplemental Fig. S8C). The conditions for immunoblotting and color development were as described previously (Shen et al., 2010).

Coimmunoprecipitation and Immunoselection Experiments

For immunoprecipitation analysis, 6-d-old seedlings were harvested, ground into fine powder in liquid nitrogen (100 mg of each sample), and then mixed with 200 μL of cold immunoprecipitation buffer (50 mM Tris, pH 7.5, 100 mM NaCl, 10% [v/v] glycerol, with freshly made protease inhibitors, 1 μM leupeptin and 2 mM pepstatin A, and 1 mM phenylmethylsulfonyl fluoride; Isono and Schwechheimer, 2010) and kept on ice for 20 min. The extraction solution was then centrifuged at 13,000g for 20 min at 4°C. The supernatant was transferred to a fresh tube. The protein concentration was determined using the Bio-Rad protein assay system (Bradford, 1976). The protein concentration was adjusted to a final concentration of 2 to 3 μg μL^{-1}, and 1 mg of total proteins was typically used for each immunoprecipitation. Ten microliters of PP2A-A antibodies was added into the extracts and kept rotating for 2 h at 4°C, followed by adding 50 μL of prewashed protein A-agarose beads. After another 2 h rotating in 4°C, the agarose-immune complex were then precipitated at 6,000g for 1 min and washed three times in cold immunoprecipitation buffer. The pellets were mixed with 2× SDS sample loading buffer (62.5 mM Tris-Cl, 1% [w/v] SDS, 10% [v/v] glycerol, 100 mM DTT, and 0.01% [w/v] Bromphenol Blue, pH 6.8). The samples were then boiled for 10 min and centrifuged at 13,000g for 1 min to remove the protein A-agarose beads. The samples were resolved by 12% SDS-PAGE and subjected to immunoblot analysis.

For immunoselection experiments, 1 mg of total protein extracts with a concentration of 1 μg μL^{-1} from different genetic backgrounds was applied to glutathione-agarose beads that bind to GST fusion proteins. After 2 h of rotation at 4°C, the beads were washed three times with phosphate-buffered saline (pH 7.4) for 10 min each. The beads were centrifuged at 13,000g for 2 min and then boiled in 1× SDS loading buffer for 5 min before being separated by 12% (w/v) SDS-PAGE.

PP2A Activity Assay

Protein extracts from 6-d-old seedlings under normal growth conditions were used for PP2A activity assay. The commercial kit for PP2A activity assay, the Ser/Thr Phosphatase Assay System from Promega, was used in this study. The procedure for the PP2A assay as outlined by the manufacturer's instruction manual was followed by using the phosphorylated polypeptide RRA(pT)VA as substrate. In addition, a chelator of divalent ions (EDTA) was included in the protein phosphatase reaction buffer (50 mM Tris-HCl, pH 7, 0.1 mM Na$_2$EDTA, 5 mM DTT, and 0.01% [w/v] Brij 35) to inhibit the activity of PP2C and other divalent-dependent phosphatases. Protein Phosphatase Inhibitor 2 from New England Biolabs was also supplemented in the reaction buffer to specifically inhibit the activity of PP1. PP2A activity was defined as pmol phosphate released from the substrates per min per μg total protein. Three independent experiments were conducted.

Sequence information for genes used in this article can be found in the Arabidopsis Genome Initiative database with the following accession numbers: At4g08960 (*AtPTPA*), At1g25490 (*RCN1*), At3g25800 (*PP2A-A2*), At1g13320 (*PP2A-A3*), At1g02100 (*SBI1*), At3g26020 (*ATB' η*), At4g15415 (*ATB' γ*), At2g01980 (*SOS1*), and At5g03280 (*EIN2*).

Supplemental Data

The following materials are available in the online version of this article.

Supplemental Figure S1. Protein sequence comparison.

Supplemental Figure S2. Transcript analysis of *AtPTPA* in wild-type and amiR plants.

Supplemental Figure S3. Transcript analysis of *AtPTPA* in wild-type, *rcn1-6* mutant, and three independent amiR (*rcn1-6*) plants and Western blot analyses of AtPTPA and PP2Ac in *rcn1-6* mutant and two independent amiR (*rcn1-6*) plants.

Supplemental Figure S4. Phenotypes and leaf numbers of the wild type and various mutants and transgenic plants.

Supplemental Figure S5. Germination rates of wild-type, *rcn1-6*, and amiR (*rcn1-6*) plants in the presence of ABA and NaCl, respectively.

Supplemental Figure S6. Real-time quantitative PCR analyses of expression of *ABI5* and *ABI5* downstream genes in wild-type and amiR plants.

Supplemental Figure S7. Characterization of *GFP-AtPTPA* transgenic plants.

Supplemental Figure S8. Characterization of AtPTPA antibodies, PP2Ac total and PP2Ac methylation specific antibodies, and the specificity of PP2Ac methylation-specific antibodies.

Supplemental Table S1. The sequence information of oligonucleotide primers used in this research.

LITERATURE CITED

Alonso JM, Hirayama T, Roman G, Nourizadeh S, Ecker JR (1999) EIN2, a bifunctional transducer of ethylene and stress responses in Arabidopsis. Science **284:** 2148–2152

Ballesteros I, Domínguez T, Sauer M, Paredes P, Duprat A, Rojo E, Sanmartín M, Sánchez-Serrano JJ (2013) Specialized functions of the PP2A subfamily II catalytic subunits PP2A-C3 and PP2A-C4 in the distribution of auxin fluxes and development in Arabidopsis. Plant J **73:** 862–872

Blakeslee JJ, Zhou HW, Heath JT, Skottke KR, Barrios JA, Liu SY, DeLong A (2008) Specificity of RCN1-mediated protein phosphatase 2A regulation in meristem organization and stress response in roots. Plant Physiol **146:** 539–553

Bradford MM (1976) A rapid and sensitive method for the quantitation of microgram quantities of protein utilizing the principle of protein-dye binding. Anal Biochem **72:** 248–254

Bryant JC, Westphal RS, Wadzinski BE (1999) Methylated C-terminal leucine residue of PP2A catalytic subunit is important for binding of regulatory Balpha subunit. Biochem J **339:** 241–246

Cayla X, Goris J, Hermann J, Hendrix P, Ozon R, Merlevede W (1990) Isolation and characterization of a tyrosyl phosphatase activator from rabbit skeletal muscle and Xenopus laevis oocytes. Biochemistry **29:** 658–667

Chao Y, Xing Y, Chen Y, Xu Y, Lin Z, Li Z, Jeffrey PD, Stock JB, Shi Y (2006) Structure and mechanism of the phosphotyrosyl phosphatase activator. Mol Cell **23:** 535–546

Chen J, Martin BL, Brautigan DL (1992) Regulation of protein serine-threonine phosphatase type-2A by tyrosine phosphorylation. Science **257:** 1261–1264

Clough SJ, Bent AF (1998) Floral dip: a simplified method for Agrobacterium-mediated transformation of *Arabidopsis thaliana*. Plant J **16:** 735–743

DeLong A (2006) Switching the flip: protein phosphatase roles in signaling pathways. Curr Opin Plant Biol **9:** 470–477

Farkas I, Dombrádi V, Miskei M, Szabados L, Koncz C (2007) Arabidopsis PPP family of serine/threonine phosphatases. Trends Plant Sci **12:** 169–176

Fellner T, Lackner DH, Hombauer H, Piribauer P, Mudrak I, Zaragoza K, Juno C, Ogris E (2003) A novel and essential mechanism determining specificity and activity of protein phosphatase 2A (PP2A) *in vivo*. Genes Dev **17:** 2138–2150

Finkelstein RR, Gampala SS, Rock CD (2002) Abscisic acid signaling in seeds and seedlings. Plant Cell (Suppl) **14:** S15–S45

Finkelstein RR, Lynch TJ (2000) The *Arabidopsis* abscisic acid response gene ABI5 encodes a basic leucine zipper transcription factor. Plant Cell **12:** 599–609

Garbers C, DeLong A, Deruére J, Bernasconi P, Söll D (1996) A mutation in protein phosphatase 2A regulatory subunit A affects auxin transport in Arabidopsis. EMBO J 15: 2115–2124

Guo F, Stanevich V, Wlodarchak N, Sengupta R, Jiang L, Satyshur KA, Xing Y (2014) Structural basis of PP2A activation by PTPA, an ATP-dependent activation chaperone. Cell Res 24: 190–203

He X, Anderson JC, del Pozo O, Gu YQ, Tang X, Martin GB (2004) Silencing of subfamily I of protein phosphatase 2A catalytic subunits results in activation of plant defense responses and localized cell death. Plant J 38: 563–577

Heidari B, Matre P, Nemie-Feyissa D, Meyer C, Rognli OA, Møller SG, Lillo C (2011) Protein phosphatase 2A B55 and A regulatory subunits interact with nitrate reductase and are essential for nitrate reductase activation. Plant Physiol 156: 165–172

Hemmings BA, Adams-Pearson C, Maurer F, Müller P, Goris J, Merlevede W, Hofsteenge J, Stone SR (1990) Alpha- and beta-forms of the 65-kDa subunit of protein phosphatase 2A have a similar 39 amino acid repeating structure. Biochemistry 29: 3166–3173

Hombauer H, Weismann D, Mudrak I, Stanzel C, Fellner T, Lackner DH, Ogris E (2007) Generation of active protein phosphatase 2A is coupled to holoenzyme assembly. PLoS Biol 5: e155

Hu R, Zhu Y, Shen G, Zhang H (2014) TAP46 plays a positive role in the ABSCISIC ACID INSENSITIVE5-regulated gene expression in Arabidopsis. Plant Physiol 164: 721–734

Hunter T (1995) Protein kinases and phosphatases: the yin and yang of protein phosphorylation and signaling. Cell 80: 225–236

Isono E, Schwechheimer C (2010) Co-immunoprecipitation and protein blots. Methods Mol Biol 655: 377–387

Janssens V, Goris J (2001) Protein phosphatase 2A: a highly regulated family of serine/threonine phosphatases implicated in cell growth and signalling. Biochem J 353: 417–439

Jefferson RA, Kavanagh TA, Bevan MW (1987) GUS fusions: β-glucuronidase as a sensitive and versatile gene fusion marker in higher plants. EMBO J 6: 3901–3907

Jordens J, Janssens V, Longin S, Stevens I, Martens E, Bultynck G, Engelborghs Y, Lescrinier E, Waelkens E, Goris J, et al (2006) The protein phosphatase 2A phosphatase activator is a novel peptidyl-prolyl cis/trans-isomerase. J Biol Chem 281: 6349–6357

Kalhor HR, Luk K, Ramos A, Zobel-Thropp P, Clarke S (2001) Protein phosphatase methyltransferase 1 (Ppm1p) is the sole activity responsible for modification of the major forms of protein phosphatase 2A in yeast. Arch Biochem Biophys 395: 239–245

Kwak JM, Moon JH, Murata Y, Kuchitsu K, Leonhardt N, DeLong A, Schroeder JI (2002) Disruption of a guard cell-expressed protein phosphatase 2A regulatory subunit, RCN1, confers abscisic acid insensitivity in Arabidopsis. Plant Cell 14: 2849–2861

Larsen PB, Chang C (2001) The Arabidopsis eer1 mutant has enhanced ethylene responses in the hypocotyl and stem. Plant Physiol 125: 1061–1073

Leivar P, Antolín-Llovera M, Ferrero S, Closa M, Arró M, Ferrer A, Boronat A, Campos N (2011) Multilevel control of Arabidopsis 3-hydroxy-3-methylglutaryl coenzyme A reductase by protein phosphatase 2A. Plant Cell 23: 1494–1511

Leulliot N, Vicentini G, Jordens J, Quevillon-Cheruel S, Schiltz M, Barford D, van Tilbeurgh H, Goris J (2006) Crystal structure of the PP2A phosphatase activator: implications for its PP2A-specific PPIase activity. Mol Cell 23: 413–424

Li YM, Casida JE (1992) Cantharidin-binding protein: identification as protein phosphatase 2A. Proc Natl Acad Sci USA 89: 11867–11870

Liu H, Stone SL (2010) Abscisic acid increases Arabidopsis ABI5 transcription factor levels by promoting KEG E3 ligase self-ubiquitination and proteasomal degradation. Plant Cell 22: 2630–2641

Longin S, Jordens J, Martens E, Stevens I, Janssens V, Rondelez E, De Baere I, Derua R, Waelkens E, Goris J, et al (2004) An inactive protein phosphatase 2A population is associated with methylesterase and can be reactivated by the phosphotyrosyl phosphatase activator. Biochem J 380: 111–119

Lopez-Molina L, Mongrand S, Chua NH (2001) A postgermination developmental arrest checkpoint is mediated by abscisic acid and requires the ABI5 transcription factor in Arabidopsis. Proc Natl Acad Sci USA 98: 4782–4787

Michniewicz M, Zago MK, Abas L, Weijers D, Schweighofer A, Meskiene I, Heisler MG, Ohno C, Zhang J, Huang F, et al (2007) Antagonistic regulation of PIN phosphorylation by PP2A and PINOID directs auxin flux. Cell 130: 1044–1056

Muday GK, Brady SR, Argueso C, Deruère J, Kieber JJ, DeLong A (2006) RCN1-regulated phosphatase activity and EIN2 modulate hypocotyl gravitropism by a mechanism that does not require ethylene signaling. Plant Physiol 141: 1617–1629

Mumby MC, Green DD, Russell KL (1985) Structural characterization of cardiac protein phosphatase with a monoclonal antibody: evidence that the Mr = 38,000 phosphatase is the catalytic subunit of the native enzyme(s). J Biol Chem 260: 13763–13770

Ogris E, Du X, Nelson KC, Mak EK, Yu XX, Lane WS, Pallas DC (1999) A protein phosphatase methylesterase (PME-1) is one of several novel proteins stably associating with two inactive mutants of protein phosphatase 2A. J Biol Chem 274: 14382–14391

País SM, González MA, Téllez-Iñón MT, Capiati DA (2009) Characterization of potato (Solanum tuberosum) and tomato (Solanum lycopersicum) protein phosphatases type 2A catalytic subunits and their involvement in stress responses. Planta 230: 13–25

Pérez-Callejón E, Casamayor A, Pujol G, Camps M, Ferrer A, Ariño J (1998) Molecular cloning and characterization of two phosphatase 2A catalytic subunit genes from Arabidopsis thaliana. Gene 209: 105–112

Pernas M, García-Casado G, Rojo E, Solano R, Sánchez-Serrano JJ (2007) A protein phosphatase 2A catalytic subunit is a negative regulator of abscisic acid signalling. Plant J 51: 763–778

Pilet PE, Saugy M (1987) Effect on root growth of endogenous and applied IAA and ABA: a critical reexamination. Plant Physiol 83: 33–38

Ron D, Dressler H (1992) pGSTag: a versatile bacterial expression plasmid for enzymatic labeling of recombinant proteins. Biotechniques 13: 866–869

Ruediger R, Roeckel D, Fait J, Bergqvist A, Magnusson G, Walter G (1992) Identification of binding sites on the regulatory A subunit of protein phosphatase 2A for the catalytic C subunit and for tumor antigens of simian virus 40 and polyomavirus. Mol Cell Biol 12: 4872–4882

Schwab R, Ossowski S, Riester M, Warthmann N, Weigel D (2006) Highly specific gene silencing by artificial microRNAs in Arabidopsis. Plant Cell 18: 1121–1133

Shen G, Kuppu S, Venkataramani S, Wang J, Yan J, Qiu X, Zhang H (2010) ANKYRIN REPEAT-CONTAINING PROTEIN 2A is an essential molecular chaperone for peroxisomal membrane-bound ASCORBATE PEROXIDASE3 in Arabidopsis. Plant Cell 22: 811–831

Shi H, Ishitani M, Kim C, Zhu JK (2000) The Arabidopsis thaliana salt tolerance gene SOS1 encodes a putative Na^+/H^+ antiporter. Proc Natl Acad Sci USA 97: 6896–6901

Skottke KR, Yoon GM, Kieber JJ, DeLong A (2011) Protein phosphatase 2A controls ethylene biosynthesis by differentially regulating the turnover of ACC synthase isoforms. PLoS Genet 7: e1001370

Stanevich V, Jiang L, Satyshur KA, Li Y, Jeffrey PD, Li Z, Menden P, Semmelhack MF, Xing Y (2011) The structural basis for tight control of PP2A methylation and function by LCMT-1. Mol Cell 41: 331–342

Stanevich V, Zheng A, Guo F, Jiang L, Wlodarchak N, Xing Y (2014) Mechanisms of the scaffold subunit in facilitating protein phosphatase 2A methylation. PLoS ONE 9: e86955

Tang W, Yuan M, Wang R, Yang Y, Wang C, Oses-Prieto JA, Kim TW, Zhou HW, Deng Z, Gampala SS, et al (2011) PP2A activates brassinosteroid-responsive gene expression and plant growth by dephosphorylating BZR1. Nat Cell Biol 13: 124–131

Tung HY, Alemany S, Cohen P (1985) The protein phosphatases involved in cellular regulation. 2. Purification, subunit structure and properties of protein phosphatases-2A0, 2A1, and 2A2 from rabbit skeletal muscle. Eur J Biochem 148: 253–263

Wei H, Ashby DG, Moreno CS, Ogris E, Yeong FM, Corbett AH, Pallas DC (2001) Carboxymethylation of the PP2A catalytic subunit in Saccharomyces cerevisiae is required for efficient interaction with the B-type subunits Cdc55p and Rts1p. J Biol Chem 276: 1570–1577

Wu G, Wang X, Li X, Kamiya Y, Otegui MS, Chory J (2011) Methylation of a phosphatase specifies dephosphorylation and degradation of activated brassinosteroid receptors. Sci Signal 4: ra29

Wu J, Tolstykh T, Lee J, Boyd K, Stock JB, Broach JR (2000) Carboxyl methylation of the phosphoprotein phosphatase 2A catalytic subunit promotes its functional association with regulatory subunits in vivo. EMBO J 19: 5672–5681

Zhou HW, Nussbaumer C, Chao Y, DeLong A (2004) Disparate roles for the regulatory A subunit isoforms in Arabidopsis protein phosphatase 2A. Plant Cell 16: 709–722